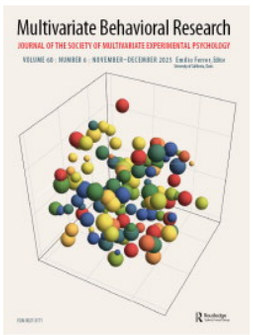

Multivariate Behavioral Research

ISSN: 0027-3171 (Print) 1532-7906 (Online) Journal homepage: www.tandfonline.com/journals/hmbr20

# Moderating the Consequences of Longitudinal Change for Distal Outcomes

Ethan M. McCormick

**To cite this article:** Ethan M. McCormick (14 Jan 2026): Moderating the Consequences of Longitudinal Change for Distal Outcomes, Multivariate Behavioral Research, DOI: 10.1080/00273171.2026.2613311

**To link to this article:** https://doi.org/10.1080/00273171.2026.2613311

MULTIVARIATE BEHAVIORAL RESEARCH
https://doi.org/10.1080/00273171.2026.2613311



# Moderating the Consequences of Longitudinal Change for Distal Outcomes

Ethan M. McCormick[a,b]

[a]Education Statistics and Research Methods, School of Education, University of Delaware, Newark, Delaware, USA; [b]Methodology & Statistics Department, Institute of Psychology, Leiden University, Leiden, Netherlands

**ABSTRACT**

There has been a growing interest in using earlier change to predict downstream distal outcomes in development; however, prior work has mostly focused on estimating the unique effect of the different growth parameters (e.g., intercept and slope) rather than focusing on the trajectory as a whole. Here I lay out a distal outcome latent curve model with latent interactions which attempts to model the *joint* effect of growth parameters on these later outcomes. I show again that these models require us to contend with unintuitive time coding effects which can impact the direction and significance of effects and that plotting and probing are necessary for disambiguating these joint effects. These graphical approaches emphasize practical steps for applied researchers in understanding these effects. I then outline how future research can help clarify optimal approaches for using the trajectory as a whole rather than the unique effects of its individual sub-components.

**KEYWORDS**

Latent curve model; distal outcome; latent interaction; time coding; regions of significance

## Introduction

The latent curve model (LCM) is a flexible framework for modeling individual differences in change over time (Bollen & Curran, 2006; Grimm et al., 2016; Meredith & Tisak, 1990), and incorporating the effect of time-invariant and time-varying predictors (Biesanz et al., 2004; Curran et al., 2004; McCormick et al., 2023; McNeish & Matta, 2020). In developmental and clinical applications, however, researchers are often interested in not only the *course* and *causes* of change, but also the *consequences* for later distal outcomes (Curran et al., 2010). This latter extension of the latent curve model has received less attention (but see Muthén and Curran (1997); Seltzer et al. (1997); von Soest and Hagtvet (2011)) and involves the use of the growth process itself to predict distal outcomes (i.e., the consequences of developmental change). In recent work (McCormick et al., 2024), we formally laid out the model for a latent curve model with distal outcomes, investigated the role of time coding for the parameters of the model, and proposed methods for optimally estimating the distal outcome predictive relationships (Feng & Hancock, 2022; Hancock & Choi, 2006). Here, I expand this approach to consider the *joint* effect of the growth factors *via* latent moderation within the distal outcome LCM framework and explore how it can help bridge a conceptual divide between a holistic characterization of change over time and the downstream consequences of development.

Our prior work focused on models with additive effects of the growth factors on distal outcomes, with our primary concern being obtaining maximally interpretable unique estimates of each factor controlling for the other (McCormick et al., 2024). This additive specification is straightforward and familiar from regression contexts, but can be conceptually limiting when the substantive focus is on overall patterns of change rather than the unique contribution of each factor. That is, while we can obtain unique parameter estimates to characterize each growth factor and its respective effects, they fundamentally measure different aspects of the same thing: the holistic trajectory of developmental change. Below, I contrast this main effects approach with another factor model context where we might wish to predict some distal outcome to make this point more clearly.

Consider a longitudinal study of the effects of adolescent anxiety and depression on substance use during adulthood. While we would similarly regress

**CONTACT** Ethan M. McCormick emccorm@udel.edu Education Statistics and Research Methods, School of Education, University of Delaware, Newark, DE, USA; Methodology & Statistics Department, Institute of Psychology, Leiden University, Leiden, Netherlands

Supplemental data for this article can be accessed online at https://doi.org/10.1080/00273171.2026.2613311.
The code required to reproduce all analysis can be found at https://osf.io/a5ruy/

substance use on the two (likely correlated) factors, fundamentally, the two latent factors are defined by different items and measurement structures. By contrast, we estimate both intercepts and slopes from the same set of items in the growth model (albeit with strictly defined rather than estimated factor loadings), and both factors *jointly* characterize an individual's trajectory over time. In this light, obtaining unique effects on a distal outcome seems a poor conceptual fit to the idea of using individual differences in growth as a whole to predict downstream consequences. Unique effects are also limited if we expect theoretical differences in the effect of increases or decreases in some behavior based on its initial or average level. For instance, the consequences of adolescence-specific increases in antisocial behavior very likely differ for teens starting with low baseline levels compared with teens already showing heightened negative behaviors. In each of these cases in particular, a holistic understanding of change is necessary to contextualize the distal outcome relationship.

One potential alternative for capturing such joint patterns is the growth mixture or latent class approach (Bauer & Reyes, 2010; Jung & Wickrama, 2008; Muthén & Muthén, 2000; Nagin, 1999), which posits latent subgroups with qualitatively-distinct overall patterns of change. These subgroups are often named based on joint trajectory information, with common examples being "high-stable" or "low-increasing" (Sher et al., 2011). Latent class models have well-developed techniques for predicting outcomes from using class membership (e.g., Li et al., 2001; Nylund-Gibson et al., 2019), and are attractive when qualitatively different "kinds" of trajectories are expected (Bauer & Curran, 2003; Bauer & Reyes, 2010). However, these models also present several challenges, including returning inappropriate group solutions (Bauer, 2007; Bauer & Curran, 2003; Hipp & Bauer, 2006; Sher et al., 2011), difficulties in class enumeration (Kim, 2014; Nylund et al., 2007), and a propensity to discretize continuous heterogeneity in growth (e.g., returning stacked "high", "medium", and "low" classes).

In cases of continuous heterogeneity, a continuous bilinear interaction has an attractive theoretical match to the idea of joint prediction of the distal outcome from the trajectory of change as a whole without assuming discrete classes. Namely, capturing how the effect of one feature of the trajectory (e.g., the slope) varies as a function of another (e.g., the intercept). To model all these effects, I lay out a moderated distal outcome latent curve model where the joint effect of the growth factors is used as an additional predictor in an attempt to bring greater conceptual clarity between prior growth and downstream consequences. I consider two potential approaches to estimating latent interactions and contrast their performance in a series of targeted simulations to assess the feasibility of estimating these latent moderation models. Next, given the inferential challenges associated with time coding decisions in the main effects model (McCormick et al., 2024), I also evaluate the potential estimation and inferential challenges in this expanded model related to intercept placement. As expected, the attendant complications are expanded in the moderated distal outcome LCM, and so I extend a set of tools used to evaluate moderation effects graphically and demonstrate a method for obtaining maximally interpretable joint effects. I conclude with a demonstration of these principles in real data and a set of recommendations for researchers in applied settings.

## Latent interactions

Interactions are a key component in the application of the multiple regression model (Aiken & West, 1991), and have been used extensively to assess how the effect of a target predictor changes across levels of another predictor (or set of predictors in high-order interactions). In the context of latent curve models, there has been extensive development of methods for probing and plotting interactions that arise as a function of conditioning the growth factors on a set of predictors (Curran et al., 2004; Preacher et al., 2006). Interactions also arise in structural equation models more broadly in multiple-groups models (Jöreskog, 1971; Sörbom, 1974) and their generalization in moderated nonlinear factor models (Bauer, 2017; Bauer & Hussong, 2009). However, these interactions differ in one fundamental point from those we might consider here in that they involve at least one observed variable as a constituent of the product term. By contrast, we are interested in estimating the interaction effect of two unobserved latent factors. While many of the principles of specifying, probing, and plotting these latent interactions remain familiar from their observed variable counterparts, there are additional estimation challenges we need to take into consideration. Below, I begin by specifying the latent interaction growth model with distal outcomes, and then consider two alternative approaches for estimating this model.

### *Latent interaction growth models with distal outcomes*

We can specify the latent interaction model (Figure 1) by expanding the main effects model I outlined in

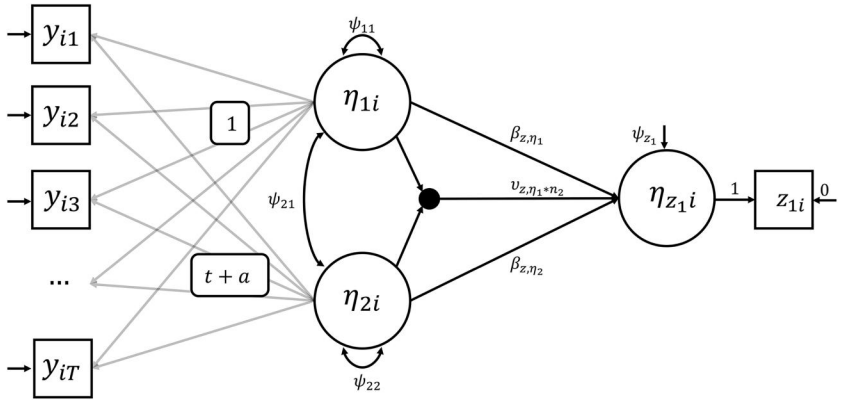


**Figure 1.** Latent Interaction Model. The distal outcome ($z_{1i}$; specified by a single-indicator factor $\eta_{z_1 i}$) is modeled as a function of the intercept ($\eta_{1i}$) and slope ($\eta_{2i}$) of the growth process of the observed repeated measures ($y_{ti}$), as well as their bilinear interaction ($\eta_{1i}\eta_{2i}$; small black circle with arrows extending from both factors). Factor loadings for $y_{ti}$ are summarized as 1's for the intercept and linearly increasing values of time ($t$) centered through some shift value ($a$).

McCormick et al. (2024). I briefly recapitulate the general LCM with distal outcomes structure here and then move on to incorporate the latent interaction. For a vector of repeatedly-assessed outcome variables $\mathbf{y}_i$ for individual $i = 1, 2, ..., N$ at time $t = 1, 2, ..., T$, we can define a latent growth process with the measurement structure

$$\mathbf{y}_i = \mathbf{\Lambda}\boldsymbol{\eta}_i + \boldsymbol{\varepsilon}_i \tag{1}$$

with $\mathbf{\Lambda}$ as a $T \times K$ matrix of factor loadings of the intercept ($\lambda_{t,1} = 1 \ \forall \ t$) and powered values of time ($t$) for $k = 1, 2, ..., K$ latent growth factors, $\boldsymbol{\eta}_i$ as a $K$-length vector of latent factors, and $\boldsymbol{\varepsilon}_i$ as a $T$-length vector of time-specific residuals of $\mathbf{y}_i$, which are distributed as $\boldsymbol{\varepsilon}_i \sim MVN(0, \mathbf{\Theta})$. The structural model inter-relating the growth factors and distal outcome(s) is defined as

$$\boldsymbol{\eta}_i = \boldsymbol{\alpha} + \mathbf{B}\boldsymbol{\eta}_i + \boldsymbol{\zeta}_i \tag{2}$$

where the $K$-length vector $\boldsymbol{\eta}_i$ is defined by a $K$-length vector of factor intercepts ($\boldsymbol{\alpha}$) and a $K$-length vector of factor disturbances ($\boldsymbol{\zeta}_i$) which are distributed as $\boldsymbol{\zeta}_i \sim MVN(0, \mathbf{\Psi})$, and are inter-related with $\mathbf{B}$, a lower-triangular $K \times K$ matrix of regression coefficients. For the inclusion of the distal outcomes into the model, we can expand the $K$-length vector $\boldsymbol{\eta}_i$ to include additional factors in the structural model $\boldsymbol{\eta}_{z,i}$ which are related to the $P$-length vector of observed distal outcomes through an indicator factor approach ($\lambda_{z_p, \eta_{z,i}} = 1$) or for multiple-indicator latent factors through a more-conventional measurement structure. As an example, we can consider a linear latent growth curve model defined by 5 repeated measures with a single distal outcome and expand our matrix expressions in Equation 1 and 2 to define the measurement model as

$$\begin{bmatrix} y_{1i} \\ y_{2i} \\ y_{3i} \\ y_{4i} \\ y_{5i} \\ z_{1i} \end{bmatrix} = \begin{bmatrix} 1 & 0 & 0 \\ 1 & 1 & 0 \\ 1 & 2 & 0 \\ 1 & 3 & 0 \\ 1 & 4 & 0 \\ 0 & 0 & 1 \end{bmatrix} \begin{bmatrix} \eta_{1i} \\ \eta_{2i} \\ \eta_{z_1 i} \end{bmatrix} + \begin{bmatrix} \varepsilon_{1i} \\ \varepsilon_{2i} \\ \varepsilon_{3i} \\ \varepsilon_{4i} \\ \varepsilon_{5i} \\ \varepsilon_{z_1 i} \end{bmatrix} \tag{3}$$

with covariance matrix $\mathbf{\Theta}$ for $\boldsymbol{\varepsilon}_i$. Note that $y_{ti}$ and $z_{pi}$ appear in the same outcome vector but are related by the factor loadings to distinct factors—$\eta_{1i}$ (the intercept) and $\eta_{2i}$ (the slope) for $y_{ti}$, and $\eta_{pi}$ for the distal outcome ($z_{pi}$). At the structural level, we can partition the relationships between the factors in $\boldsymbol{\eta}_i$ by specifying unique covariance blocks among the growth factors and distal outcome factors separately in $\mathbf{\Psi}$, and structuring the relationships between the growth factors and distal outcome factors as regressions in $\mathbf{B}$. The expanded structural model would be

$$\begin{bmatrix} \eta_{1i} \\ \eta_{2i} \\ \eta_{z_1 i} \end{bmatrix} = \begin{bmatrix} \alpha_1 \\ \alpha_2 \\ \alpha_{z_1} \end{bmatrix} + \begin{bmatrix} 0 & 0 & 0 \\ 0 & 0 & 0 \\ \beta_{z_1,\eta_1} & \beta_{z_1,\eta_2} & 0 \end{bmatrix} \begin{bmatrix} \eta_{1i} \\ \eta_{2i} \\ \eta_{z_1 i} \end{bmatrix} + \begin{bmatrix} \zeta_{1i} \\ \zeta_{2i} \\ \zeta_{z_1 i} \end{bmatrix} \tag{4}$$

with a covariance matrix of $\mathbf{\Psi}$ with the form

$$\mathbf{\Psi} = \begin{bmatrix} \psi_{11} & \psi_{12} & 0 \\ \psi_{21} & \psi_{22} & 0 \\ 0 & 0 & \psi_z \end{bmatrix} \tag{5}$$

with zeros on the block off-diagonals to avoid redundancy with the regression coefficients in $\mathbf{B}$. The model-implied moment structure—mean $\boldsymbol{\mu}(\boldsymbol{\theta})$ and covariance matrix $\mathbf{\Sigma}(\boldsymbol{\theta})$—can then be expressed using standard notation (e.g., Bollen, 1989) as

$$\begin{aligned} \boldsymbol{\mu}(\boldsymbol{\theta}) &= \mathbf{\Lambda}\boldsymbol{\alpha} \\ \mathbf{\Sigma}(\boldsymbol{\theta}) &= \mathbf{\Lambda}(\mathbf{I} - \mathbf{B})^{-1}\mathbf{\Psi}(\mathbf{I} - \mathbf{B})^{-1'}\mathbf{\Lambda}' + \mathbf{\Theta} \end{aligned} \tag{6}$$

With this foundation in place, we can then consider a model which expands these expressions to include a bilinear interaction between the intercept and slope growth factors as an additional predictor of the distal outcome. Here we expand Equation 2 to include the latent interaction as

$$\boldsymbol{\eta}_i = \boldsymbol{\alpha} + \mathbf{B}\boldsymbol{\eta}_i + \mathbf{D}\boldsymbol{\eta}_i'\boldsymbol{\Upsilon}\,\boldsymbol{\eta}_i + \boldsymbol{\zeta}_i \tag{7}$$

where $\boldsymbol{\Upsilon}$ψis a $K \times K$ upper-triangular matrix of regression coefficients associated with latent interactions among endogenous latent variables ($\boldsymbol{\eta}_i$), with quadratic effects on the diagonal (e.g., $\eta_{2i}^2$), and bilinear effects on the off-diagonal (e.g., $\eta_{1i}\eta_{2i}$). In the example distal outcome growth model above, this would take the form

$$\boldsymbol{\Upsilon} = \begin{bmatrix} 0 & \upsilon_{12} & 0 \\ 0 & 0 & 0 \\ 0 & 0 & 0 \end{bmatrix} \tag{8}$$

to indicate the bilinear effect of $\eta_{1i}$ and $\eta_{2i}$ ($\upsilon_{12}$). The $K \times 1$ indicator matrix $\mathbf{D}$ controls the target of the latent interaction(s) for a given element in $\boldsymbol{\eta}_i$. For example

$$\mathbf{D} = \begin{bmatrix} 0 \\ 0 \\ 1 \end{bmatrix} \tag{9}$$

indicates that $\upsilon_{12}$ targets the distal outcome factor ($\eta_{z_1 i}$). In the model we have outlined thus far, we only need a single $\boldsymbol{\Upsilon}$ψand $\mathbf{D}$ matrix to model the joint effect of the latent growth factors on the one distal outcome; however, for additional distal outcomes (or generally additional interaction effects on any other factors), we would need to specify a series of $\boldsymbol{\Upsilon}$ψmatrices targeting different variables in $\boldsymbol{\eta}_i$. For $P$ interaction targets, Equation 7 takes a more general notation of

$$\boldsymbol{\eta}_i = \boldsymbol{\alpha} + \mathbf{B}\boldsymbol{\eta}_i + \sum_{p=1}^{P} \mathbf{D}_p\left(\boldsymbol{\eta}_i'\boldsymbol{\Upsilon}_p\boldsymbol{\eta}_i\right) + \boldsymbol{\zeta}_i \tag{10}$$

Note that in Equation 10 we only model the effects of interactions—including the possibility of quadratic effects—between *endogenous* latent variables, however, we could also use a similar formulation to model interactions between *exogenous* latent variables ($\boldsymbol{\xi}_i$) with a set of $K \times K$ upper-triangular matrices $\boldsymbol{\Omega}$ (Kelava et al., 2011), and between endogenous and exogenous latent variables with a set of $K \times K$ upper-triangular matrices $\boldsymbol{\Pi}$ (Jin et al., 2021). Each $p$ interaction target is modeled with a unique set of matrices $\mathbf{D}$, $\boldsymbol{\Upsilon}$, $\boldsymbol{\Pi}$, and $\boldsymbol{\Omega}$ with the relevant interaction effects for that outcome target.

$$\boldsymbol{\eta}_i = \boldsymbol{\alpha} + \mathbf{B}\boldsymbol{\eta}_i + \sum_{p=1}^{P} \mathbf{D}_p\left(\boldsymbol{\eta}_i'\boldsymbol{\Upsilon}_p\boldsymbol{\eta}_i + \boldsymbol{\xi}_i'\boldsymbol{\Pi}_p\boldsymbol{\eta}_i + \boldsymbol{\xi}_i'\boldsymbol{\Omega}_p\boldsymbol{\xi}_i\right) + \boldsymbol{\zeta}_i \tag{11}$$

While alternative formulations for latent interactions exist (see Jin et al., 2021), this relatively simple additive form will be useful for clarifying the derivations of time coding effect that I outline in the following section.

By conventions of model path diagrams, we can visualize the latent interaction as a small, solid circle with arrows pointing to it from the constituent growth factors (Figure 1). We can then represent the effect of the latent interaction on the distal outcome ($\upsilon_{z,\eta_1*\eta_2}$) with an additional regression arrow. This bilinear effect of $\eta_{1i}\eta_{2i}$ then represents the change in the main effect of one factor per unit change in the other. Because of the primary theoretical interest in the predictive effect of the slope on the distal outcome, I will interpret this bilinear effect primarily as a measure of how the predictive effect of the slope factor changes at different levels of the intercept factor (although the interaction is of course symmetric). While here I present the simple linear growth model with a single distal outcome, this model could be straightforwardly expanded to include nonlinear growth factors and multiple distal outcomes using Equation 10 and 11 (see Appendix for an expanded explication in these expanded models).

## Estimation approaches

There have been a variety of approaches proposed for estimating latent interaction historically including product indicators (Foldnes & Hagtvet, 2014; Kenny & Judd, 1984), latent moderated structural equations (LMS; Klein & Moosbrugger, 2000; Moosbrugger et al., 2009), and two-step Structural After Measurement (SAM; Li et al., 2000; Rosseel & Loh, 2024) approaches. Neither the LMS nor the SAM approach require observed product indicators, which is especially useful in the growth context, where we do not have distinct sets of indicators to create products from—rather, the interaction needs to be estimated directly out of the latent variables defined by a single set of indicators. The LMS approach is derived under the assumption of joint multivariate normality of all latent variables and residuals, and models the non-normality inherent in an interaction term through a finite Gaussian mixture approximation (for technical details, see Klein & Moosbrugger, 2000), while the SAM approach generates

corrected factor scores in a first measurement estimation step, and creates an observed product interaction in the second structural model estimation step (Rosseel & Loh, 2024). One limitation of both the LMS and SAM approaches is the lack of standard fit indices to evaluate the model. The standard saturated model is not an appropriate baseline for the nonlinear factor model using the LMS approach (Kelava et al., 2011); thus, proper $\chi^2$ goodness-of-fit tests cannot be performed, and all associated fit indices (e.g., CFI, TLI, RMSEA, etc.) are unreliable. Likewise, the second-step SAM model is often just-identified with no parameter constraints, and also limits fit-based evaluations of the predictions of the distal outcome. As such, here I will primarily focus on parameter recovery, and will rely on the Bayesian Information Criteria (BIC) when model comparisons are necessary.

Because the LMS approach relies on joint multivariate normality, it is sensitive to the distributional specification of the latent variables in particular (Klein & Moosbrugger, 2000; Lonati et al., 2025), and multivariate tests of the observed indicators and Hausman tests of the latent variables are recommended in practice (Lonati et al., 2025) to ensure conformation to these assumptions. The SAM approach, by contrast, avoids these distributional assumptions through the use of observed scores to create the product term. To focus this investigation on the conceptual use-case of latent interactions for predicting distal outcomes from the trajectory as a whole and potential issues of time coding, the main simulations here conform to the LMS assumption of joint normality. A set of simulations on the recovery of the LMS and SAM on data generated with (weakly) non-normal latent variables (marginally distributed as Gumbel variates) are presented in the Supplemental Material. As expected, the LMS results are compromised under these data conditions, especially with respect to the standard error estimates.

## Evaluating LMS versus SAM performance

To evaluate whether the two estimation approaches appropriately capture the interaction effect of the growth factors on the distal outcomes as expected, I simulated data from the following population moments,

$$\boldsymbol{\alpha} = \begin{bmatrix} 3 & 0.2 \end{bmatrix} \qquad \boldsymbol{\Psi}_{std} = \begin{bmatrix} 1 & 0.15 & 0 \\ 0.15 & 1 & 0 \\ 0 & 0 & 1 \end{bmatrix}$$

$$\mathbf{B} = \begin{bmatrix} 0 & 0 & 0 \\ 0 & 0 & 0 \\ 0.2 & 0.1 & 0 \end{bmatrix} \quad \boldsymbol{\Upsilon} = \begin{bmatrix} 0 & 0.05 & 0 \\ 0 & 0 & 0 \\ 0 & 0 & 0 \end{bmatrix},$$

and fit the resulting data with both the one-step LMS (Moosbrugger et al., 2009), and the two-step Structural After Measurement (SAM; Rosseel & Loh, 2024) approach using the specified bilinear interaction LCM with distal outcomes. For all models, I estimated the intercept at the first repeated measure ($\lambda_{12} = 0$). To systematically evaluate the recovery of the latent interaction effects under various conditions, I simulated data while varying the following design factors: the sample size $n \in \{100, 250, 500\}$, and the number of repeated measures observations $t \in \{3, 5\}$ to define the growth factors. For each of 1000 simulated data sets, I fit the model in three ways: 1) the latent moderated structural equation (LMS) approach in `Mplus`, 2) the Structural After Measurement (SAM) approach with naive standard errors in `lavaan`, and 3) the SAM approach with bootstrapped standard errors (1000 bootstrap samples). The results for parameter recovery can be seen in Table 1, and the results for standard error recovery can be seen in Table 2 (all code required to replicate these results is available in the Supplemental Material).

The recovery of parameter estimates for the target distal outcome regression was similar for both the LMS and SAM approaches in terms of the average

**Table 1.** Parameter Recovery: LMS and SAM Estimates.

| | | LMS Estimates | | | SAM Estimates | | |
|---|---|---|---|---|---|---|---|
| | | $n = 100$ | $n = 250$ | $n = 500$ | $n = 100$ | $n = 250$ | $n = 500$ |
| | | $r = 854/997$ | $r = 976/1000$ | $r = 997/1000$ | $r = 1000/1000$ | $r = 1000/1000$ | $r = 1000/1000$ |
| $\beta_{z,\eta_1} = 0.20$ | $t = 3$ | 0.198 (0.081) | 0.204 (0.058) | 0.202 (0.036) | 0.194 (0.125) | 0.194 (0.088) | 0.199 (0.050) |
| | $t = 5$ | 0.204 (0.063) | 0.200 (0.036) | 0.201 (0.026) | 0.205 (0.075) | 0.201 (0.039) | 0.201 (0.027) |
| $\beta_{z,\eta_2} = 0.10$ | $t = 3$ | 0.136 (0.480) | 0.124 (0.235) | 0.113 (0.172) | 0.127 (1.28) | 0.042 (0.870) | 0.097 (0.436) |
| | $t = 5$ | 0.083 (0.317) | 0.092 (0.182) | 0.096 (0.148) | 0.096 (0.509) | 0.102 (0.270) | 0.091 (0.186) |
| $\upsilon_{z,\eta_1\eta_2} = 0.05$ | $t = 3$ | 0.042 (0.129) | 0.036 (0.061) | 0.045 (0.048) | 0.035 (0.466) | 0.072 (0.313) | 0.050 (0.142) |
| | $t = 5$ | 0.050 (0.091) | 0.051 (0.061) | 0.050 (0.043) | 0.052 (0.157) | 0.051 (0.085) | 0.052 (0.059) |

Note: For each sample size ($n$, column) and number of repeated measures ($t$, row), the mean effect estimate is shown with the standard deviation of effects in parentheses. The number of replications that converged $r$ is indicated for $t = 3/t = 5$. The generating values for the main effect of the intercept ($\beta_{z,\eta_1}$), main effect of the slope ($\beta_{z,\eta_2}$), and bilinear interaction effect ($\upsilon_{z,\eta_1\eta_2}$) are shown in the leftmost column. There were no instances where the generating value was not contained in $\pm$ 1 SD of the average recovered effect. Monte Carlo standard errors were small ($M_{MCSE} = 0.0065$; *range* = 0.0008 – 0.0405) across effects.

**Table 2.** Standard Error Recovery: LMS and SAM Estimates.

| | | | LMS Estimates | | SAM Estimates | | |
|---|---|---|---|---|---|---|---|
| | | | $SD_{empirical}$ | S.E. | $SD_{empirical}$ | S.E.$_{naive}$ | S.E.$_{bootstrap}$ |
| $\beta_{z,\eta_1}$ | $n = 100$ | $t = 3$ | 0.081 | 0.057 (0.108) | 0.125 | **0.028 (0.014)** | 0.135 (0.065) |
| | | $t = 5$ | 0.063 | 0.044 (0.022) | 0.075 | **0.029 (0.009)** | 0.124 (0.097) |
| | $n = 250$ | $t = 3$ | 0.058 | 0.043 (0.059) | 0.088 | **0.019 (0.008)** | 0.165 (0.102) |
| | | $t = 5$ | 0.036 | 0.027 (0.010) | 0.039 | **0.018 (0.003)** | 0.044 (0.034) |
| | $n = 500$ | $t = 3$ | 0.036 | 0.026 (0.017) | 0.050 | **0.013 (0.004)** | 0.179 (0.128) |
| | | $t = 5$ | 0.026 | **0.019 (0.004)** | 0.027 | **0.013 (0.001)** | 0.022 (0.006) |
| $\beta_{z,\eta_2}$ | $n = 100$ | $t = 3$ | 0.480 | 0.300 (0.395) | 1.28 | **0.182 (0.193)** | 1.06 (0.482) |
| | | $t = 5$ | 0.317 | **0.214 (0.092)** | 0.509 | **0.177 (0.068)** | 0.981 (0.760) |
| | $n = 250$ | $t = 3$ | 0.235 | 0.192 (0.150) | 0.870 | **0.118 (0.132)** | 1.39 (0.752) |
| | | $t = 5$ | 0.182 | **0.136 (0.034)** | 0.270 | **0.108 (0.025)** | 0.333 (0.343) |
| | $n = 500$ | $t = 3$ | 0.172 | 0.134 (0.064) | 0.436 | **0.082 (0.056)** | 1.62 (1.10) |
| | | $t = 5$ | 0.148 | **0.096 (0.017)** | 0.186 | **0.075 (0.012)** | 0.150 (0.055) |
| $\upsilon_{z,\eta_1\eta_2}$ | $n = 100$ | $t = 3$ | 0.129 | 0.080 (0.054) | 0.466 | **0.060 (0.059)** | 0.337 (0.144) |
| | | $t = 5$ | 0.091 | 0.065 (0.024) | 0.157 | **0.055 (0.023)** | 0.328 (0.253) |
| | $n = 250$ | $t = 3$ | 0.061 | 0.051 (0.024) | 0.313 | **0.039 (0.042)** | 0.452 (0.240) |
| | | $t = 5$ | 0.060 | **0.042 (0.011)** | 0.085 | **0.034 (0.008)** | 0.107 (0.110) |
| | $n = 500$ | $t = 3$ | 0.048 | 0.037 (0.012) | 0.142 | **0.026 (0.019)** | 0.526 (0.335) |
| | | $t = 5$ | 0.043 | **0.030 (0.005)** | 0.059 | **0.024 (0.004)** | 0.047 (0.018) |

Note: For each sample size ($n$) and number of repeated measures ($t$), the empirical standard deviation ($SD_{empirical}$; from Table 1) of effects is compared with the average standard error (S.E.) estimate, with the standard deviation of recovered S.E.s in parentheses. Instances where the $SD_{empirical}$ was not contained in $\pm$ 1 SD of the average recovered S.E. are bolded. The results are organized by effect, including the main effect of the intercept ($\beta_{z,\eta_1}$), main effect of the slope ($\beta_{z,\eta_2}$), and bilinear interaction effect ($\upsilon_{z,\eta_1\eta_2}$). Monte Carlo standard errors were small ($M_{MCSE} = 0.0054$; *range* = 0.0001 – 0.0346) across effects.

estimate, although there was greater variability in the SAM estimates across almost all conditions (see Table 1). Increasing both $t$ and $n$ improved the recovery of effects and shrank the variability of estimates, suggesting multiple avenues for improving estimates in real data. However, even at relatively low sample sizes and a minimal number of repeated measures ($n = 100$, $t = 3$), the recovered effects of the latent interaction ($\upsilon_{z,\eta_1\eta_2}$) were reasonable, especially for the LMS approach, suggesting that probing for the latent interaction effect is feasible in many applied settings. By contrast, the recovery of the main effect of the slope ($\beta_{z,\eta_2}$) was poorest among all the considered effects, especially at low $n$ and $t$, which may be related to the relatively extreme value of $\eta_{1i} = 0$ (compared with $\alpha_1 = 3$) it is evaluated at.

For the standard errors, the greater efficiency of the LMS approach (in a properly specified model)[1] is evident compared to the SAM approaches (naive vs. bootstrap SEs), with much smaller variability in recovered effects. The LMS standard error estimates approximated the empirical variability in the recovered effect estimates well in most conditions for this model specification, although it tended to show too-small standards errors at higher sample sizes ($n = 250$ and 500) and number of repeated measures ($t = 5$). The SAM approaches diverged in expected ways. The naive standard errors in the two-stage SAM approach substantially underestimated the empirical variability, while the bootstrap approach corrected for the increased uncertainty in recovered effects. Indeed, the bootstrap approach sometimes *over-corrected*, with a higher average SE estimate than the empirical variability, although the true variability was almost always contained within one standard deviation of S.E.s recovered. Both the LMS and bootstrap SAM approaches underestimated the uncertainty of the bilinear interaction in the smallest sample size ($n = 100$) and number of repeated measures ($t = 3$).

[1]See the Supplemental Material for a brief simulation with non-Gaussian latent variables, where the LMS recovery of standard errors is compromised compared with the bootstrap SAM approach.

### *Time coding effects in the latent interaction model*

The inferential challenge of time coding influences on parameter recovery is well documented in the general (Biesanz et al., 2004) and main effects distal outcome (McCormick et al., 2024) latent curve model, and for many parameters, the time coding relationships have been previously defined. For a given set of data with two different time coding schemes (e.g., intercept at the first and the final time point), we can define a transformation matrix **T** which relates the factor loading matrices of the two models. In a linear growth model, **T** has the form

$$\mathbf{T} = \begin{bmatrix} 1 & a \\ 0 & b \end{bmatrix} \tag{13}$$

where $a$ moves the location of the intercept through addition (see Figure 1) and $b$ scales the slope through multiplication with the factor loadings. For purposes of this treatment, I assume that $b = 1$. For consistency with the single-indicator latent factor approach I used

in Figure 1, I expand $\mathbf{T}$ by 1 dimension with 1's on the diagonal and zeros otherwise

$$\mathbf{T} = \begin{bmatrix} 1 & a & 0 \\ 0 & b = 1 & 0 \\ 0 & 0 & 1 \end{bmatrix} \tag{14}$$

Using this expanded matrix, the results of any one model solution can be transformed into another, resulting in a transformed factor loading matrix ($\boldsymbol{\Lambda}^*$)

$$\boldsymbol{\Lambda}^* = \boldsymbol{\Lambda}\mathbf{T} \tag{15}$$

a transformed covariance matrix ($\boldsymbol{\Psi}^*$)

$$\boldsymbol{\Psi}^* = \mathbf{T}^{-1}\boldsymbol{\Psi}\mathbf{T}^{-1'} \tag{16}$$

with the inverse transformation matrix ($\mathbf{T}^{-1}$)

$$\mathbf{T}^{-1} = \left(\boldsymbol{\Lambda}^{*'}\boldsymbol{\Lambda}^*\right)^{-1}\boldsymbol{\Lambda}^{*'}\boldsymbol{\Lambda} \tag{17}$$

and mean vector ($\boldsymbol{\alpha}^*$)

$$\boldsymbol{\alpha}^* = \mathbf{T}^{-1}\boldsymbol{\alpha} \tag{18}$$

and with a transformed matrix of regression coefficients of the growth factors on the distal outcome(s)[2]

$$\mathbf{B}^* = \mathbf{B}\mathbf{T} \tag{19}$$

To incorporate latent interactions into this time coding framework, I derived a similar expression to transform between interaction parameter estimates obtained under two given time coding schemes, which results in the following equality (see Appendix for detailed derivations)

$$\boldsymbol{\Upsilon}^* = \mathbf{T}'\boldsymbol{\Upsilon}\mathbf{T} \tag{20}$$

Using $\mathbf{T}$ from Equation 14 with $a = -4$ and $\upsilon_{21} = 0.05$, I show that with an original

$$\boldsymbol{\Upsilon}^* = \begin{bmatrix} \upsilon_{11} & \upsilon_{12} & 0 \\ 0 & \upsilon_{22} & 0 \\ 0 & 0 & 0 \end{bmatrix} = \begin{bmatrix} 0 & 0.05 & 0 \\ 0 & 0 & 0 \\ 0 & 0 & 0 \end{bmatrix} \tag{21}$$

then $\boldsymbol{\Upsilon}^*$ is

$$\begin{aligned} \boldsymbol{\Upsilon}^* = \mathbf{T}'\boldsymbol{\Upsilon}\mathbf{T} &= \begin{bmatrix} 1 & 0 & 0 \\ -4 & 1 & 0 \\ 0 & 0 & 1 \end{bmatrix}\begin{bmatrix} 0 & 0.05 & 0 \\ 0 & 0 & 0 \\ 0 & 0 & 0 \end{bmatrix}\begin{bmatrix} 1 & -4 & 0 \\ 0 & 1 & 0 \\ 0 & 0 & 1 \end{bmatrix} \\ &= \begin{bmatrix} 0 & 0.05 & 0 \\ 0 & -0.2 & 0 \\ 0 & 0 & 0 \end{bmatrix} \end{aligned} \tag{22}$$

Two points of interest emerge out of this quadratic expression. First, the bilinear interaction effect of the growth factors is time coding invariant, such that

$$\upsilon_{12}^* = \upsilon_{12} \tag{23}$$

However, the point of concern is that in order to maintain the equality expressed in Equation 22 and 23, a quadratic effect ($\upsilon_{22} = -0.2$) of the slope growth factor ($\eta_{2i}^2$) emerges—an effect we do not specify in the theoretical model (Figure 1). Like the main effect of the slope ($\beta_{z,\eta_2}$) itself, which I showed in McCormick et al. (2024) changes linearly across different time codings as a function of the main effect of the intercept ($\beta_{z,\eta_1}$)

$$\beta_{z,\eta_2}^* = \beta_{z,\eta_2} + \beta_{z,\eta_1}\Delta a, \tag{24}$$

the quadratic effect of the slope ($\upsilon_{z,\eta_2^2}$) changes linearly as a function of the bilinear interaction effect of the intercept and slope ($\upsilon_{z,\eta_1\eta_2}$).

$$\upsilon_{z,\eta_2^2}^* = \upsilon_{z,\eta_2^2} + \upsilon_{z,\eta_1\eta_2}\Delta a \tag{25}$$

This means that unless this additional quadratic effect is specified during model estimation, the likelihood equivalency between the two models is lost, and the effect of the bilinear interaction on the distal outcome ($\upsilon_{12}^*$) is nonequivalent—and therefore biased—in alternative time coding models. In Figure 2, I plot the estimates of the latent interaction effect ($\hat{\upsilon}_{z,\eta_1\eta_2}$) from models with the intercept coded at $t = 1, 2, \ldots, 5$, with the point estimate and 95% confidence intervals in comparison with the population generating value ($\upsilon_{z,\eta_1\eta_2} = 0.05$). Failing to include the quadratic effect of the slope ($\upsilon_{z,\eta_2^2}$) in these models biases the recovered estimates of the bilinear interaction effect downwards as we move away from the time coding approach where $\upsilon_{z,\eta_2^2} = 0$ (here at $t = 1$; see the Supplemental Material for full results).

These time coding relationships only get more complex if we consider the full matrix of interaction effect—namely the addition of the quadratic effect of the intercept. The time coding effects in Equation 22 and 25 only hold if $\upsilon_{11} = 0$. Otherwise, the time coding transformations are as follows.

$$\begin{aligned} \boldsymbol{\Upsilon}^* = \mathbf{T}'\boldsymbol{\Upsilon}\mathbf{T} &= \begin{bmatrix} 1 & 0 & 0 \\ a & b & 0 \\ 0 & 0 & 0 \end{bmatrix}\begin{bmatrix} \upsilon_{11} & \upsilon_{12} & 0 \\ 0 & \upsilon_{22} & 0 \\ 0 & 0 & 0 \end{bmatrix}\begin{bmatrix} 1 & a & 0 \\ 0 & b & 0 \\ 0 & 0 & 0 \end{bmatrix} \\ &= \begin{bmatrix} \upsilon_{11} & \upsilon_{11}a + \upsilon_{12}b & 0 \\ \upsilon_{11}a & \upsilon_{11}a^2 + \upsilon_{12}ab + \upsilon_{22}b^2 & 0 \\ 0 & 0 & 0 \end{bmatrix} \end{aligned} \tag{26}$$

[2]Note that this notation differs slightly from prior work (McCormick et al., 2024) which simplified $z_i$ as an observed outcome. Both approaches give the same results; the matrices are only adjusted to maintain conformability.

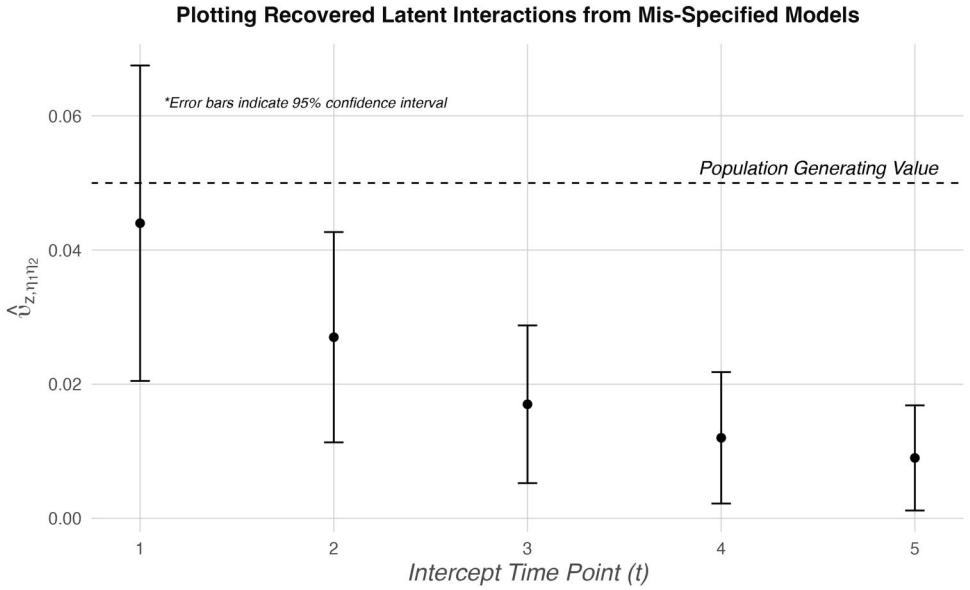


**Figure 2.** Latent Interaction Estimates from Mis-Specified Alternative Time Coding Models. When only including the bilinear interaction effect, altering the time coding scheme results in nonequivalent effect estimates. In particular, as the time coding moves away from the scheme in the generating model (here this means forward in the longitudinal design), the bilinear effect is biased downwards toward zero.

which simplifies to

$$\boldsymbol{\Upsilon}^* = \begin{bmatrix} \upsilon_{11} & \upsilon_{11}a + \upsilon_{12} & 0 \\ \upsilon_{11}a & \upsilon_{11}a^2 + \upsilon_{12}a + \upsilon_{22} & 0 \\ 0 & 0 & 0 \end{bmatrix} \tag{27}$$

when $b = 1$.

In this expanded model, $\upsilon_{11}$ is the only truly time coding invariant parameter in $\boldsymbol{\Upsilon}\psi$(and likewise $\pi_{11}$ in $\boldsymbol{\Pi}$ and $\omega_{11}$ in $\boldsymbol{\Omega}$ if these matrices are included). Even more troubling is that when $\upsilon_{11} \neq 0$, these time coding transformations violate the upper-triangular structure of $\boldsymbol{\Upsilon}\psi$ as originally defined, with $\boldsymbol{\Upsilon}^*_{12} = \upsilon_{11}a$ and $\boldsymbol{\Upsilon}^*_{21} = \upsilon_{11}a + \upsilon_{12}$. Both elements imply an effect of the bilinear interaction of $\eta_1\eta_2$ on the distal outcome ($z$), and when modeled with observed data, it should be impossible to obtain separate estimates for these parameters. In practice, we should expect that the obtained parameter estimates will combine these two transformations with the following expression.

$$\upsilon^*_{z,\eta_1\eta_2} = \upsilon_{z,\eta_1\eta_2} + 2\upsilon_{z,\eta_1^2}\Delta a \tag{28}$$

However, to focus the discussion here on the parameter of interest—the bilinear interaction term—in subsequent examples, I will consider the case where $\upsilon_{11} = 0$, allowing for simplified transformations for the bilinear interaction

$$\upsilon^*_{z,\eta_1\eta_2} = \upsilon_{z,\eta_1\eta_2} \tag{29}$$

and the quadratic effect of the slope

$$\upsilon^*_{z,\eta_2^2} = \upsilon_{z,\eta_2^2} + \upsilon_{z,\eta_1\eta_2}\Delta a \tag{30}$$

hold.

### Reevaluating LMS versus SAM performance in the presence of the quadratic slope effect

I re-ran a subset of the simulations in Section 2.3, including a quadratic effect of the slope during model estimation. Given the results in Table 2, I only report the SAM models with the bootstrap standard errors here. Table 3 reports the mean ($M_{Est.}$; compare to the population generating parameter at left) and variability ($SD_{Est.}$) of the recovered parameter estimates, as well as the average recovered standard error ($M_{S.E.}$; compare to $SD_{Est.}$). The results were substantively similar for the $t = 3$ and $t = 5$ conditions, with both approaches showing unbiased average parameter estimates for the main effect of the intercept ($\beta_{z,\eta_1}$) and two interaction terms ($\upsilon_{z,\eta_1\eta_2}$ and $\upsilon_{z,\eta_2\eta_2}$); as with the bilinear-only model, the recovery of the main effect of the slope ($\beta_{z,\eta_2}$) was substantially worse. The LMS approach showed smaller standard errors compared with the SAM approach.[3] ; however, both approaches showed worse estimation of the sampling variability (captured by the $M_{S.E.}$ column) compared with the

[3]As expected in data that conform to joint normality.

**Table 3.** Model Recovery with a Quadratic Slope Effect ($n = 250$): LMS and SAM Estimates.

| | | LMS Estimates $n = 250$ $r = 945/1000$ | | SAM Estimates (bootstrap S.E.) $n = 250$ $r = 1000/1000$ | |
|---|---|---|---|---|---|
| | | $M_{Est.}$ ($SD_{Est.}$) | $M_{S.E.}$ ($SD_{S.E.}$) | $M_{Est.}$ ($SD_{Est.}$) | $M_{S.E.}$ ($SD_{S.E.}$) |
| $\beta_{z,\eta_1} = 0.20$ | $t = 3$ | 0.201 (0.052) | 0.036 (0.038) | 0.204 (0.106) | 0.138 (0.070) |
| | $t = 5$ | 0.201 (0.037) | 0.028 (0.010) | 0.203 (0.045) | 0.097 (0.093) |
| $\beta_{z,\eta_2} = 0.10$ | $t = 3$ | 0.122 (0.332) | 0.219 (0.204) | 0.051 (0.989) | 1.14 (0.582) |
| | $t = 5$ | 0.103 (0.209) | 0.148 (0.047) | 0.086 (0.324) | 0.880 (0.797) |
| $\upsilon_{z,\eta_1\eta_2} = 0.05$ | $t = 3$ | 0.045 (0.113) | 0.076 (0.079) | 0.057 (0.348) | 0.363 (0.175) |
| | $t = 5$ | 0.047 (0.071) | **0.050 (0.019)** | 0.051 (0.111) | 0.349 (0.316) |
| $\upsilon_{z,\eta_2\eta_2} = 0.00$ | $t = 3$ | 0.006 (0.208) | 0.140 (0.208) | 0.009 (0.624) | 0.548 (0.264) |
| | $t = 5$ | 0.001 (0.095) | 0.073 (0.037) | 0.000 (0.139) | 0.495 (0.449) |

Note: For the sample size $n = 250$ and number of repeated measures ($t$, row), the mean effect estimate ($M_{Est.}$) is shown with the standard deviation of effects ($SD_{Est.}$) in parentheses, followed by the mean ($M_{S.E.}$) and standard deviation ($SD_{S.E.}$) of the standard error. The number of replications that converged $r$ is indicated for $t = 3/t = 5$. The results are organized by effect, and organized by the generating values for the main effect of the intercept ($\beta_{z,\eta_1}$), main effect of the slope ($\beta_{z,\eta_2}$), bilinear interaction effect ($\upsilon_{z,\eta_1\eta_2}$), and quadratic effect of the slope ($\upsilon_{z,\eta_2\eta_2}$) shown in the leftmost column. In most instances, the generating value was contained in ± 1 SD of the average recovered effect. Instances where the generating value or the empirical *SD* was not contained in ± 1 SD are bolded.

simpler bilinear only model, although still within ± 1 SD of the sampling variability of recovered mean estimates ($SD_{Est.}$ column) for almost all conditions.

## Visualizing time coding-dependent latent interactions

I noted earlier the inferential advantages of plotting and probing these effects, similar to familiar methods for evaluating bilinear interactions in observed variables (Aiken & West, 1991). To visualize the latent interaction effect across different available time codings, I used the transformation functions outlined above to estimate the predicted effect across an arbitrary number of alternative models. However, visualizing these relationships is not entirely straightforward. While each of the latent interactions—the bilinear ($\eta_1\eta_2$) and quadratic slope ($\eta_2^2$) effects—are two-way interaction effects, the pattern of changes in parameter estimates across different time codings means that we need to adopt techniques common in three-way interaction effects. Here, I consider two different approaches for visualizing the latent interactions among growth factors.

### *Simple slopes*

In the latent interaction model, we must contend with the fact that we have both time coding *and* true interaction effects that need to be probed and plotted. As such, while they differ in their estimation, the effects here resemble a 3-way interaction in traditional regression contexts. As such, we have several options for plotting the resulting effects, depending on which feature we wish to highlight. I first use a familiar simple-slopes approach (Aiken & West, 1991; Bauer & Curran, 2005; Curran et al., 2004), where I plot the expected values of the outcome ($z$) as a function of the latent slope factor ($\eta_2$). Figure 3 displays this approach, where the different regression lines represent the expected effect of $\eta_2$ at different levels of $\eta_1$. Because we do not directly observe the values of the intercept or slope, I instead probe this interaction at model-implied levels of the intercept (i.e., the mean and ± 1 SD). I then display different simple slopes for a subset of time points ($t$) in separate panels (Figure 3). Given the slope's theoretical importance in understanding the consequences of change (McCormick et al., 2024), I evaluated the effect of $\eta_2$ at different values of $\eta_1$ across integer values of $t$,[4] however like observed interactions, the latent interaction is symmetric and I could equivalently highlight the effect of $\eta_1$ if that was of interest.

Here the presence of the negative quadratic effect of the slope becomes more pronounced as we move the intercept time point ($t$) forward in the longitudinal design, although the bilinear interaction terms maintain a constant positive influence on the main effect of the slope. Note that even at $t = 1$, there is some curvature to the simple slopes lines, in contrast to the initial models (Table 1), where I did not estimate a quadratic slope effect. However, like the aperture (Hancock & Choi, 2006; McCormick et al., 2024) minimizes the covariance between the slope and intercept in the main effects only model, it is possible to use the results of any single time coding model to estimate a time point where the quadratic effect of the slope is zero, and only the bilinear interaction remains. Indeed the formula to find this point falls

[4]Note that integer values are simply a convenient heuristic, but that the time coding transformations can be applied across any real value of $t$. Nevertheless, for practical reasons, $t$ should most often be bounded between 1 and $T$.

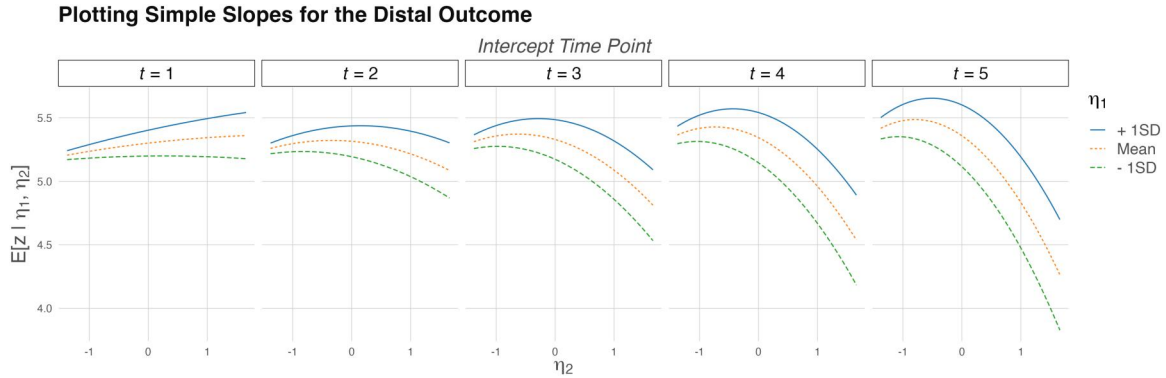


**Figure 3.** Visualizing the Latent Interaction with Simple Slopes. The model-implied values of the distal outcome ($z$) are plotted against values of the slope ($\eta_{2i}$; x-axis) for model-implied values of the intercept ($\eta_{1i}$) at the mean and $\pm$ 1 standard deviation (separate trend lines), across different time coding schemes (separate panels). Note that as the coded intercept moves forward, the quadratic slope effect induces additional curvature to the model-implied expected value trend lines. In this example, these simple slopes show that the magnitude of the effect of the slope on the distal outcome increases at higher levels of the intercept.

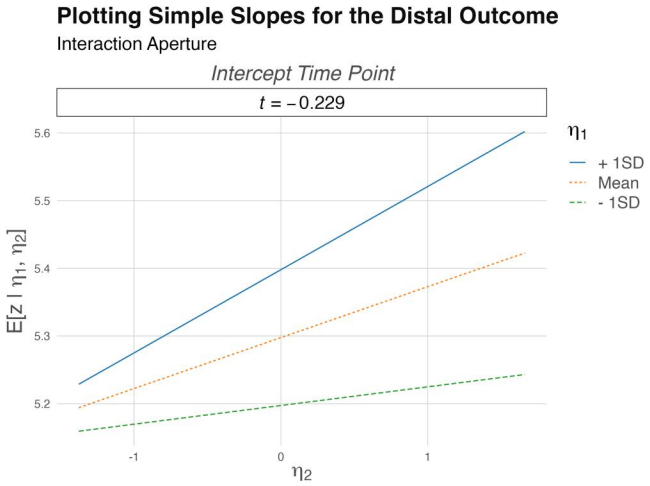


**Figure 4.** Visualizing the Latent Interaction Aperture using Simple Slopes. By estimating the moderated distal outcome growth model at the interaction aperture, we can eliminate the curvature induced by the quadratic slope effect, leaving only the simple bilinear interaction effect to interpret.

directly out of Equation 30 and has a parallel structure to that of the aperture, with the following form

$$a = \frac{-\upsilon_{z,\eta_2^2}}{\upsilon_{z,\eta_1\eta_2}} \tag{31}$$

Thus by adjusting each of the factor loadings from any estimated solution by substituting this value of $a$ (in this simulated example, $a = 0.229$) into the transformation matrix from Equation 14, we can obtain a solution where $\upsilon^*_{z,\eta_2^2} = 0$, resulting in no curvature to the model-implied simple slopes (Figure 4). For the simulated example data, this implies and interaction aperture 0.229 time units *before* the first measurement occasion. Note that this is *not* identical to the covariance aperture (Hancock & Choi, 2006), which is at $a = -0.340$ in these same data.

Like the covariance aperture, this interaction aperture is not constrained to only include values that occur within the observed time range. As such, while the interaction aperture is an attractive time point to estimate the model intercept for theoretical reasons, it is likely inadvisable in real data contexts to estimate the intercept outside the range of the data in order to protect the reliability and validity of model inferences.

## Regions of significance

An alternative to the simple slopes approach is to adopt a regions of significance plot (i.e., Johnson-Neyman plots; Johnson & Neyman, 1936) to help characterize how the regression effects of the latent interactions on the distal outcome change across alternative time codings. Similar to the main effect of the intercept and slope on the distal outcome in the model without latent interactions (see Figure 2; McCormick et al., 2024), here there is a clear contrast

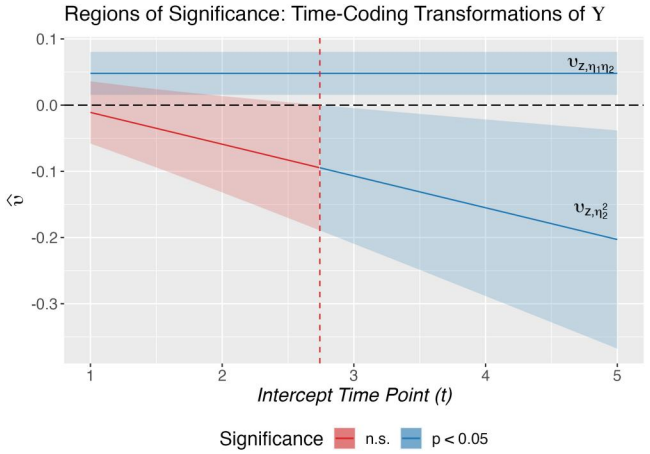


**Figure 5.** Visualizing Time Coding Changes in the Latent Interaction using Zones of Significance. Using a zones of significance approach, we can visualize the time coding-related changes in the quadratic slope effect $\upsilon_{z,\eta_2^2}$ as it changes linearly across different time coding schemes, going from non-significant to significant (at $p < 0.05$) when the intercept is placed at or after $t = 2.75$.

of how time coding changes impact the effect of the bilinear interaction ($\upsilon_{z,\eta_1\eta_2}$) and the quadratic effect of the slope factor ($\upsilon_{z,\eta_2^2}$). In Figure 5, I highlight that the point estimate and standard errors for both the effect of the bilinear interaction ($\hat{\upsilon}_{z,\eta_1\eta_2}$) are time coding invariant (again so long as we include $\upsilon_{z,\eta_2^2}$ in the model—failing to do so will lead to changes in $\hat{\upsilon}_{z,\eta_1\eta_2}$ due to misspecification; see Figure 2). In contrast, the estimated quadratic effect of the slope $\hat{\upsilon}_{z,\eta_2^2}$ changes linearly across different potential intercept time points ($t$), just as expected. Note a key difference in this plot from traditional regions of significance plots: the standard errors do not show the usual pronounced quadratic shape because the transformations are deterministic. Similar to prior work (McCormick et al., 2024), this approach shows the potential for the sign and significance of the quadratic effect to depend on the time coding scheme adopted (Figure 5).

The regions of significance plot also locates where within the time point range the quadratic slope effect will be zero (and therefore result in Figure 4), right before the start of the study period. It further shows that the effect of the bilinear interaction is invariant to time coding choices, so long as the quadratic slope is included in the model. In the next section, I will turn to an empirical example using real sample data to highlight how these approaches operate in practice.

## Real data example

To highlight the complexities I have outlined above in a real-data context, I drew publicly available data from the Tennessee's Student Teacher Achievement Ratio (STAR; Word et al., 1990; Achilles et al., 2008, data retrieved from https://doi.org/10.7910/DVN/SIWH9F) project ($n = 772$), including a maximum number of 4 repeated measures per individual ($mode = 3$) from the 5th to the 8th grade. I consider here a model where growth is estimated on repeated measures of math achievement over 4 years with a distal outcome of overall grades at the end of high school (measured on a 1–100 scale; centered prior to analysis). Prior to fitting the model, I centered the repeated measures of math achievement using the 5th grade mean and divided by 10 to rescale all variables to aid convergence.

I first fit a distal outcome latent curve model with *only* the bilinear latent interaction effect (i.e., Figure 1). To assess the impact of different time coding schemes, I chose two (of a theoretically infinite set) standard schemes often deployed in practice: 1) an initial status model (i.e., intercept at the first time point), and 2) and average status model (i.e., intercept at the middle of the trajectory). Comparing these two solutions allows us to see both the impact of time coding decisions and of the exclusion of the quadratic effect in real and incomplete data.

The results of the bilinear-only models are presented in Table 4. While the differences are slight, we can see that the initial status model ($\ell = -5874.75$) and average status model ($\ell = -5874.79$) are not likelihood-equivalent, and the effect of the bilinear latent interaction is attenuated ($\upsilon_{z,\eta_1\eta_2} = 0.642$ vs. 0.718), mirroring the simulated example (Figure 2). I then fit the same time coding schemes, but with the quadratic interaction of the slope ($\eta_2^2$) included as an additional predictor of the distal outcome (Table 5).

As expected, the key differences are that now the two alternative time coding models are likelihood equivalent ($\ell = -5874.47$) and the effect of the latent bilinear interaction is constant ($\upsilon_{z,\eta_1\eta_2} = 1.298 \ \forall \ a$) while the effect

**Table 4.** Parameter Recovery: Bilinear Effect Only.

| | Initial Status | | | | Average Status | | | |
|---|---|---|---|---|---|---|---|---|
| | $l$ | | BIC | | $l$ | | BIC | |
| | −5874.75 | | 11842.58 | | −5874.79 | | 11842.67 | |
| | Est. | S.E. | Std. Est. | $p$ | Est. | S.E. | Std. Est. | $p$ |
| $\beta_{z,\eta_1}$ | 1.697 | 1.559 | 0.938 | 0.276 | 1.785 | 1.463 | 1.063 | 0.222 |
| $\beta_{z,\eta_2}$ | −34.254 | 11.927 | −1.190 | 0.004 | −38.963 | 10.542 | −1.355 | < 0.001 |
| $\upsilon_{z,\eta_1\eta_2}$ | 0.718 | 0.377 | 0.096 | 0.057 | 0.642 | 0.355 | 0.093 | 0.071 |
| $\alpha_{\eta_1}$ | −1.749 | 0.193 | −0.453 | < 0.001 | 0.522 | 0.165 | 0.126 | 0.002 |
| $\alpha_{\eta_2}$ | 1.514 | 0.066 | 6.238 | < 0.001 | 1.513 | 0.066 | 6.228 | < 0.001 |
| $\psi_{11}$ | 14.912 | 1.538 | 1* | < 0.001 | 17.302 | 1.169 | 1* | < 0.001 |
| $\psi_{21}$ | 0.753 | 0.330 | | 0.023 | 0.851 | 0.383 | | 0.026 |
| $\rho_{21}$ | 0.803 | 0.190 | | < 0.001 | 0.842 | 0.140 | | < 0.001 |
| $\psi_{22}$ | 0.059 | 0.041 | 1* | 0.154 | 0.059 | 0.040 | 1* | 0.138 |

**Note:** $\ell$ is the log-likelihood. BIC is the Bayesian Information Criterion. Est. is the sample-recovered parameter. S.E. is the standard error of the estimate. Std. Est. is the standardized estimate. Beta ($\beta$) denotes main effects regression coefficients associated with the latent growth factors, upsilon ($\upsilon$) denotes the regression coefficients associated with the latent interaction, alpha ($\alpha$) denotes factor means, psi ($\psi$) denotes factor variances and covariances, and rho ($\rho$) denotes the factor correlation. *Denotes a constrained parameter (not estimated).

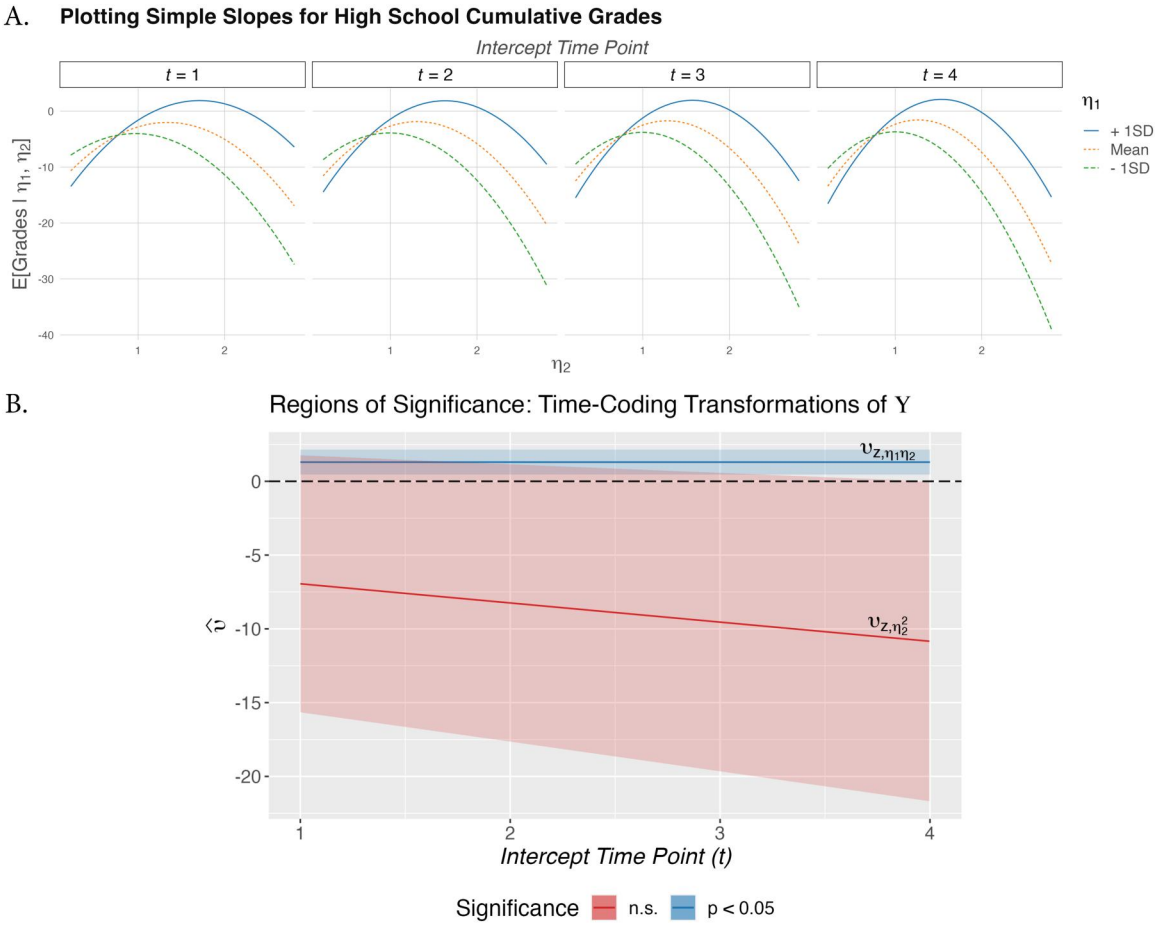


**Figure 6.** Time Coding Results for Cumulative High School Grades. While the zones of significance plot (B) highlights that the quadratic slope effect is never significant within the range of the repeated measures data, the magnitude of the effect nevertheless induces considerable curvature into the simple slopes plot (A). The positive bilinear interaction $\upsilon_{z,\eta_1\eta_2}$ suggests that higher initial math performance ($\eta_1$) boosts the impact of gains in math performance ($\beta_{z,\eta_2}$) on high school grades ($z$).

of the latent quadratic slope changes linearly (initial status $\upsilon_{z,\eta_2\eta_2} = -6.946$; average status $\upsilon_{z,\eta_2\eta_2} = -8.893$; $\Delta\upsilon_{z,\eta_2\eta_2} = -1.948 = -1.5 * 1.298$). Below, I plot the simple slopes and Johnson-Neyman regions of significance approaches to probing these effects for the distal outcome of cumulative high school grades and how they interact with the choice of time coding.

As can be seen in Figure 6(B), while the latent quadratic slope effect ($\hat{\upsilon}_{z,\eta_2^2}$) is never significant within the range of observation, it is nevertheless quite large

**Table 5.** Parameter Recovery: Bilinear and Quadratic Effects.

| | Initial Status | | | | Average Status | | | |
|---|---|---|---|---|---|---|---|---|
| | $l$ | | BIC | | $l$ | | BIC | |
| | −5874.47 | | 11848.66 | | −5874.47 | | 11848.66 | |
| | Est. | S.E. | Std. Est. | $p$ | Est. | S.E. | Std. Est. | $p$ |
| $\beta_{z,\eta_1}$ | −0.997 | 0.685 | −0.575 | 0.145 | −0.997 | 0.685 | −0.605 | 0.145 |
| $\beta_{z,\eta_2}$ | 20.887 | 13.778 | 1.306 | 0.130 | 22.380 | 14.616 | 1.400 | 0.126 |
| $\upsilon_{z,\eta_1\eta_2}$ | 1.298 | 0.430 | 0.322 | 0.003 | 1.299 | 0.430 | 0.339 | 0.003 |
| $\upsilon_{z,\eta_2\eta_2}$ | −6.946 | 4.435 | −0.187 | 0.117 | −8.893 | 4.968 | −0.239 | 0.073 |
| $\alpha_{\eta_1}$ | −1.753 | 0.192 | −0.442 | $< 0.001$ | 0.518 | 0.164 | 0.124 | 0.002 |
| $\alpha_{\eta_2}$ | 1.514 | 0.065 | 3.520 | $< 0.001$ | 1.514 | 0.065 | 3.520 | $< 0.001$ |
| $\psi_{11}$ | 15.736 | 1.419 | 1* | $< 0.001$ | 17.406 | 1.175 | 1* | $< 0.001$ |
| $\psi_{21}$ | 0.418 | 0.282 | | 0.139 | 0.695 | 0.342 | | 0.042 |
| $\rho_{21}$ | 0.245 | 0.183 | | 0.180 | 0.387 | 0.157 | | 0.014 |
| $\psi_{22}$ | 0.185 | 0.116 | 1* | 0.111 | 0.185 | 0.116 | 1* | 0.111 |

**Note:** $\ell$ is the log-likelihood. BIC is the Bayesian Information Criterion. Est. is the sample-recovered parameter. S.E. is the standard error of the estimate. Std. Est. is the standardized estimate. Beta ($\beta$) denotes main effects regression coefficients associated with the latent growth factors, upsilon ($\upsilon$) denotes the regression coefficients associated with the latent interaction, alpha ($\alpha$) denotes factor means, psi ($\psi$) denotes factor variances and covariances, and rho ($\rho$) denotes the factor correlation. *Denotes a constrained parameter (not estimated).

in terms of effect size. As a result, the model-implied simple slopes display a pronounced curvature at all the evaluated intercept time points (Figure 6(A)). The regions of significance plot (Figure 6(B)) implies that the interaction aperture (where $\upsilon_{z,\eta_2^2} = 0$) is located sometime prior to the start of the study. Using Equation 31, we can see that this is indeed the case; the interaction aperture location is estimated as being 5.351 time units prior to the first observation ($\sim$ late kindergarten). As such, I chose to retain the initial status model as the most interpretable solution because it is located closest to this aperture while remaining within the window of observation.

Substantively, we can interpret the significant bilinear interaction (Figure 6(A); left-most panel) as indicating a positive synergy between high intercepts and slopes such that those with greater starting math achievement and show greater gains during middle-school have higher predicted cumulative grades in high school. Given the magnitude of the quadratic latent slope effect, there is at least the suggestion that there may be some optimal combination of intercept and slope beyond which we see performance reversals, however, those results would need to be interpreted with extreme caution given the large uncertainty (and in the solution I chose to retain, non-significance) associated with that quadratic effect.

## Recommendations for applied researchers

Adopting a theoretical perspective on using trajectories as a whole, rather than unique effects of the different components therein, is an attractive one for probing a wide range of phenomena in the behavioral and education sciences. Interactions provide a powerful lens for understanding how the effect of the intercept or slope exists in the context of other features of the model; for instance, they allow one to distinguish between those who show greater education gains from relatively low versus high baseline ability. However, the complexity of time coding effects, already challenging for interpretation when only using main effects (McCormick et al., 2024) are, perhaps unsurprisingly, magnified further with the introduction of latent interactions.

The primary issues arose from the appearance of latent quadratic effects of the slope and the intercept (in the full solution) across different time coding solutions. Because these effects are not a standard feature of the theoretical model for understanding joint impacts of individual differences in the trajectory components, applied researchers may unknowingly fail to include these effects, leaving themselves open to nonequivalent solutions depending on the inference decisions about the intercept that may change across applications (e.g., initial vs. average vs. final status). When possible, researchers may choose to estimate these models at the intercept aperture to maximize the interpretability of the bilinear interaction, but as we saw with the applied example, this is not always feasible. The plotting and probing approaches I demonstrated here (Figures 3–5) can aid in the interpretation of results in much the same ways as are often used in observed variable interactions.

One natural question that may arise is whether applied researchers can simply ignore these problematic quadratic effects because while this may result in a mis-specified model, all models are likely mis-specified to some degree in real data. This question may seem initially reasonable given the complexity of

interpreting multiple latent interactions and the computational demands of estimating these features; however, Figure 2 and the results of the real data analysis (Table 4) suggest that this simplification approach impairs the ability to detect the bilinear interaction effect of interest—resulting in deflated effect sizes. Specifically, the larger the latent quadratic slope effect *would be* if included, the more deflated the estimates of the bilinear interaction are in models that omit that quadratic effect.

The challenges of estimation here may be addressed by adopting the Structural After Measurement (SAM; Rosseel & Loh, 2024) approach, which does not require estimating the complicated mixture components needed in LMS. As such, the SAM approach can accommodate a greater number of interactions without convergence issues. One current limitation of the SAM approach; however, is that reliable standard error estimates have not yet been derived. As such, researchers interested in employing the SAM approach should manually bootstrap the standard errors directly through resampling their target data, rather than through the internal `lavaan` bootstrapping procedure—although this may change in future versions. The SAM approach with bootstrap standard errors is also more robust to distributional misspecification of the latent variables (see marginal Gumbel simulations in the Supplemental Material). Nevertheless, for a minimal number of latent interactions and latent variables that conform to the Gaussian assumptions, the LMS approach returns smaller standard errors (i.e., greater efficiency).

## Conclusions

My goal here was to explore the utility and challenges of using latent interactions to test the impact of the trajectory as a whole on distal outcomes rather than the unique effects of its constituent features (e.g., intercept and slope separately). For estimating joint effects in continuous predictors, I turned to methods for estimating latent interactions between the growth factors, with a core theoretical focus on the bilinear interaction between intercept and slope. Based on prior work (Biesanz et al., 2004; McCormick et al., 2024) highlighting the importance of considering time coding decisions for these models, I explored how these decisions would impact estimation and interpretation of effects in a moderated distal outcome latent curve model. I laid out derivations for estimating changes in model parameters across alternative time coding schemes and confirmed them in artificial and real data. These derivations revealed a concerning pattern of effects. While the primary effect of interest in these models is the bilinear interaction, Equation 22 and 26 demonstrate how latent quadratic effects appear even when not specified in the data generating model, and when omitted from the model, result in bias in the bilinear interaction effect estimate. I showed how specifying at least the latent quadratic effect of the slope allowed me to obtain a time-coding invariant bilinear interaction effect and developed plotting and probing techniques for understanding how these latent interactions impact the distal outcome.

To further develop this initial work, there is a broad scope for additional methodological developments and investigations, including both for moderated distal outcome growth models in particular, as well as models with latent interactions more broadly. First, to maintain the focus of the current work on deriving and probing the time coding transformations for the latent interaction(s), the set of simulation conditions was constrained to a small set of population models and conditions. Future work should seek to expand on these initial simulations to more fully map the robustness of the models for capturing latent interactions among the latent growth factors, including refining estimates of power across a broader range of sample sizes and number of time points, investigating the role of missing data, and for more complex nonlinear growth trajectories. For latent interaction models more generally, substantial work remains to maximize the utility of these approaches, including derivations of valid standard errors for the two-step Structural After Measurement (SAM) product estimates, investigations into robustness of methods with and without distributional assumptions (e.g., LMS vs. SAM) in truly nonlinear data (note that the simulations in the Supplemental Material only rely on marginal nonlinearity, but many more-complex nonlinear patterns are possible; see Fairchild et al. (2024); Foldnes and Grønneberg (2019, 2022); Grønneberg et al. (2022), for examples).

Finally, the central question of how to use trajectories jointly as predictors of downstream outcomes remains a fertile area of continued research. While the continuous nature of the bilinear interaction is an attractive one for understanding the context of intercept and slope, these questions could be recast in terms of a discrete set of "kinds" of different trajectories. This recasting would lend itself naturally to the estimation of latent classes of trajectories using latent class (e.g., Muthén & Muthén, 2000; Nagin, 1999) models which have distinct combinations of growth features. These latent class growth models have faced

general critiques in the past as prone to extract stereotypical or spurious classes of growth (e.g., always high/low stable, increasing, and decreasing classes; Sher et al., 2011), and these issues likely would remain in the kinds of models considered here. Nevertheless, as a method for estimating areas of high local density in multivariate space, these latent class approaches may help researchers gain better leverage in interpreting the consequences of trajectories as a whole for later developmental outcomes. One pressing question that should be addressed before adopting these approaches more broadly is the sensitivity of class size and composition to choices of time coding. If latent class solutions are robust to time coding in a way that continuous latent interactions are not, this may increase the attractiveness of these discrete latent variable approaches in distal outcome growth models. However, if features of latent class growth models (e.g., class enumeration or assignment)depend on time coding choices, then the added complexity of mixture distributions may serve to obscure rather than clarify our understanding of the downstream consequences of change over time.

## Article information

**Conflict of interest disclosures:** The author signed a form for disclosure of potential conflicts of interest. The author did not report any financial or other conflicts of interest in relation to the work described.

**Ethical principles:** The author affirms having followed professional ethical guidelines in preparing this work. These guidelines include obtaining informed consent from human participants, maintaining ethical treatment and respect for the rights of human or animal participants, and ensuring the privacy of participants and their data, such as ensuring that individual participants cannot be identified in reported results or from publicly available original or archival data.

**Funding:** EMM was supported with funds from the NWO (Nederlandse Organisatie voorWetenschappelijk Onderzoek), Domain Social Sciences and Humanities (SSH) Sector Plan: Resilience in Youth, NWO Veni (VI.Veni.231G.012), and Jacobs Foundation Fellowship (2023-1510-00).

**Role of the funders/sponsors:** None of the funders or sponsors of this research had any role in the design and conduct of the study; collection, management, analysis, and interpretation of data; preparation, review, or approval of the manuscript; or decision to submit the manuscript for publication.

**Acknowledgments:** The author would like to thank Patrick J. Curran and Gregory R. Hancock for their comments on prior versions of this manuscript. The ideas and opinions expressed herein are those of the author alone, and endorsement by the author's institutions or funding bodies is not intended and should not be inferred.

## Open scholarship

This article has earned the Center for Open Science badges for Open Data and Open Materials through Open Practices Disclosure. The data and materials are openly accessible at https://doi.org/10.7910/DVN/SIWH9F and https://osf.io/a5ruy/.

## References

Achilles, C., Bain, H. P., Bellott, F., Boyd-Zaharias, J., Finn, J., Folger, J., Johnston, J., & Word, E. (2008). Tennessee's student teacher achievement ratio (STAR) project. https://doi.org/10.7910/DVN/SIWH9F

Aiken, L. S., & West, S. G. (1991). *Multiple regression: Testing and interpreting interactions*. Sage Publications, Inc.

Bauer, D. J. (2007). Observations on the use of growth mixture models in psychological research. *Multivariate Behavioral Research*, *42*(4), 757–786. https://doi.org/10.1080/00273170701710338

Bauer, D. J. (2017). A more general model for testing measurement invariance and differential item functioning. *Psychological Methods*, *22*(3), 507–526. https://doi.org/10.1037/met0000077

Bauer, D. J., & Curran, P. J. (2003). Distributional assumptions of growth mixture models: Implications for overextraction of latent trajectory classes. *Psychological Methods*, *8*(3), 338–363. https://doi.org/10.1037/1082-989X.8.3.338

Bauer, D. J., & Curran, P. J. (2005). Probing interactions in fixed and multilevel regression: Inferential and graphical techniques. *Multivariate Behavioral Research*, *40*(3), 373–400. https://doi.org/10.1207/s15327906mbr4003_5

Bauer, D. J., & Hussong, A. M. (2009). Psychometric approaches for developing commensurate measures across independent studies: Traditional and new models. *Psychological Methods*, *14*(2), 101–125. https://doi.org/10.1037/a0015583

Bauer, D. J., & Reyes, H. L. M. (2010). Modeling variability in individual development: Differences of degree or kind? *Child Development Perspectives*, *4*(2), 114–122. https://doi.org/10.1111/j.1750-8606.2010.00129.x

Biesanz, J. C., Deeb-Sossa, N., Papadakis, A. A., Bollen, K. A., & Curran, P. J. (2004). The role of coding time in estimating and interpreting growth curve models. *Psychological Methods*, *9*(1), 30–52. https://doi.org/10.1037/1082-989X.9.1.30

Bollen, K. A. (1989). *Structural equations with latent variables*. Wiley.

Bollen, K. A., & Curran, P. J. (2006). *Latent curve models: A structural equation perspective*. John Wiley & Sons.

Curran, P. J., Bauer, D. J., & Willoughby, M. T. (2004). Testing main effects and interactions in latent curve analysis. *Psychological Methods*, *9*(2), 220–237. https://doi.org/10.1037/1082-989X.9.2.220

Curran, P. J., Obeidat, K., & Losardo, D. (2010). Twelve frequently asked questions about growth curve modeling.

*Journal of Cognition and Development: Official Journal of the Cognitive Development Society*, *11*(2), 121–136. https://doi.org/10.1080/15248371003699969

Fairchild, A. J., Yin, Y., Baraldi, A. N., Astivia, O. L. O., & Shi, D. (2024). Many nonnormalities, one simulation: Do different data generation algorithms affect study results? *Behavior Research Methods*, *56*(7), 6464–6484. https://doi.org/10.3758/s13428-024-02364-w

Feng, Y., & Hancock, G. R. (2022). Model-based incremental validity. *Psychological Methods*, *27*(6), 1039–1060. https://doi.org/10.1037/met0000342

Foldnes, N., & Grønneberg, S. (2019). On identification and non-normal simulation in ordinal covariance and item response models. *Psychometrika*, *84*(4), 1000–1017. https://doi.org/10.1007/s11336-019-09688-z

Foldnes, N., & Grønneberg, S. (2022). Non-normal data simulation using piecewise linear transforms. *Structural Equation Modeling: A Multidisciplinary Journal*, *29*(1), 36–46. https://doi.org/10.1080/10705511.2021.1949323

Foldnes, N., & Hagtvet, K. A. (2014). The choice of product indicators in latent variable interaction models: Post hoc analyses. *Psychological Methods*, *19*(3), 444–457. https://doi.org/10.1037/a0035728

Grimm, K. J., Ram, N., & Estabrook, R. (2016). *Growth modeling: Structural equation and multilevel modeling approaches*. Guilford Publications.

Grønneberg, S., Foldnes, N., & Marcoulides, K. M. (2022). Covsim: An R package for simulating non-normal data for structural equation models using copulas. *Journal of Statistical Software*, *102*(3), 1–45. https://doi.org/10.18637/jss.v102.i03

Hancock, G. R., & Choi, J. (2006). A vernacular for linear latent growth models. *Structural Equation Modeling: A Multidisciplinary Journal*, *13*(3), 352–377. https://doi.org/10.1207/s15328007sem1303_2

Hipp, J. R., & Bauer, D. J. (2006). Local solutions in the estimation of growth mixture models. *Psychological Methods*, *11*(1), 36–53. https://doi.org/10.1037/1082-989X.11.1.36

Jin, S., Noh, M., Yang-Wallentin, F., & Lee, Y. (2021). Robust nonlinear structural equation modeling with interaction between exogenous and endogenous latent variables. *Structural Equation Modeling: A Multidisciplinary Journal*, *28*(4), 547–556. https://doi.org/10.1080/10705511.2020.1857255

Johnson, P. O., & Neyman, J. (1936). Tests of certain linear hypotheses and their application to some educational problems. *Statistical Research Memoirs*, *1*, 57–93.

Jöreskog, K. G. (1971). Simultaneous factor analysis in several populations. *Psychometrika*, *36*(4), 409–426. https://doi.org/10.1007/BF02291366

Jung, T., & Wickrama, K. a S. (2008). An Introduction to latent class growth analysis and growth mixture modeling. *Social and Personality Psychology Compass*, *2*(1), 302–317. https://doi.org/10.1111/j.1751-9004.2007.00054.x

Kelava, A., Werner, C. S., Schermelleh-Engel, K., Moosbrugger, H., Zapf, D., Ma, Y., Cham, H., Aiken, L. S., & West, S. G. (2011). Advanced nonlinear latent variable modeling: Distribution analytic LMS and QML estimators of interaction and quadratic effects. *Structural Equation Modeling: A Multidisciplinary Journal*, *18*(3), 465–491. https://doi.org/10.1080/10705511.2011.582408

Kenny, D. A., & Judd, C. M. (1984). Estimating the nonlinear and interactive effects of latent variables. *Psychological Bulletin*, *96*(1), 201–210. https://doi.org/10.1037/0033-2909.96.1.201

Kim, S.-Y. (2014). Determining the number of latent classes in single- and multi-phase growth mixture models. *Structural Equation Modeling: A Multidisciplinary Journal*, *21*(2), 263–279. https://doi.org/10.1080/10705511.2014.882690

Klein, A., & Moosbrugger, H. (2000). Maximum likelihood estimation of latent interaction effects with the LMS method. *Psychometrika*, *65*(4), 457–474. https://doi.org/10.1007/BF02296338

Li, F., Duncan, T. E., & Acock, A. (2000). Modeling interaction effects in latent growth curve models. *Structural Equation Modeling: A Multidisciplinary Journal*, *7*(4), 497–533. https://doi.org/10.1207/S15328007SEM0704_1

Li, F., Duncan, T. E., Duncan, S. C., & Acock, A. (2001). Latent growth modeling of longitudinal data: A finite growth mixture modeling approach. *Structural Equation Modeling: A Multidisciplinary Journal*, *8*(4), 493–530. https://doi.org/10.1207/S15328007SEM080401

Lonati, S., Rönkkö, M., & Antonakis, J. (2025). Normality assumption in latent interaction models. *Psychological Methods*, *30*(6), 1242–1262. https://doi.org/10.1037/met0000657

McCormick, E. M., Byrne, M. L., Flournoy, J. C., Mills, K. L., & Pfeifer, J. H. (2023). The Hitchhiker's guide to longitudinal models: A primer on model selection for repeated-measures methods. *Developmental Cognitive Neuroscience*, *63*, 101281. https://doi.org/10.1016/j.dcn.2023.101281

McCormick, E. M., Curran, P. J., & Hancock, G. R. (2024). Latent growth factors as predictors of distal outcomes. *Psychological Methods*. https://doi.org/10.1037/met0000642

McNeish, D., & Matta, T. H. (2020). Flexible treatment of time-varying covariates with time unstructured data. *Structural Equation Modeling: A Multidisciplinary Journal*, *27*(2), 298–317. https://doi.org/10.1080/10705511.2019.1627213

Meredith, W., & Tisak, J. (1990). Latent curve analysis. *Psychometrika*, *55*(1), 107–122. https://doi.org/10.1007/BF02294746

Moosbrugger, H., Schermelleh-Engel, K., Kelava, A., & Klein, A. G. (2009). Testing multiple nonlinear effects in structural equation modeling: A comparison of alternative estimation approaches. In T. Teo & M. S. Khine (Eds.), *Structural Equation Modelling in Educational Research: Concepts and Applications* (pp. 1–34). Sense Publishers.

Muthén, B. O., & Curran, P. J. (1997). General longitudinal modeling of individual differences in experimental designs: A latent variable framework for analysis and power estimation. *Psychological Methods*, *2*(4), 371–402. https://doi.org/10.1037/1082-989X.2.4.371

Muthén, B. O., & Muthén, L. K. (2000). Integrating person-centered and variable-centered analyses: Growth Mixture modeling with latent trajectory classes. *Alcoholism, Clinical and Experimental Research*, *24*(6), 882–891. https://doi.org/10.1111/j.1530-0277.2000.tb02070.x

Nagin, D. S. (1999). Analyzing developmental trajectories: A semiparametric, group-based approach. *Psychological*

*Methods*, *4*(2), 139–157. https://doi.org/10.1037/1082-989X.4.2.139

Nylund, K. L., Asparouhov, T., & Muth'en, B. O. (2007). Deciding on the number of classes in latent class analysis and growth mixture modeling: A monte carlo simulation study [Publisher: Routledge eprint. *Structural Equation Modeling: A Multidisciplinary Journal*, *14*(4), 535–569. https://doi.org/10.1080/10705510701575396

Nylund-Gibson, K., Grimm, R. P., & Masyn, K. E. (2019). Prediction from latent classes: A demonstration of different approaches to include distal outcomes in mixture models. *Structural Equation Modeling: A Multidisciplinary Journal*, *26*(6), 967–985. https://doi.org/10.1080/10705511.2019.1590146

Preacher, K. J., Curran, P. J., & Bauer, D. J. (2006). Computational tools for probing interactions in multiple linear regression, multilevel modeling, and latent curve analysis. *Journal of Educational and Behavioral Statistics*, *31*(4), 437–448. https://doi.org/10.3102/10769986031004437

Rosseel, Y., & Loh, W. W. (2024). A structural after measurement approach to structural equation modeling. *Psychological Methods*, *29*(3), 561–588. https://doi.org/10.1037/met0000503

Seltzer, M. M., Greenberg, J. S., Krauss, M. W., & Hong, J. (1997). Predictors and outcomes of the end of coresident caregiving in aging families of adults with mental retardation or mental illness. *Family Relations*, *46*(1), 13–22. https://doi.org/10.2307/585602

Sher, K. J., Jackson, K. M., & Steinley, D. (2011). Alcohol use trajectories and the ubiquitous cat's cradle: Cause for concern? *Journal of Abnormal Psychology*, *120*(2), 322–335. https://doi.org/10.1037/a0021813

Sörbom, D. (1974). A general method for studying differences in factor means and factor structure between groups. *British Journal of Mathematical and Statistical Psychology*, *27*(2), 229–239. https://doi.org/10.1111/j.2044-8317.1974.tb00543.x

von Soest, T., & Hagtvet, K. A. (2011). Mediation analysis in a latent growth curve modeling framework. *Structural Equation Modeling: A Multidisciplinary Journal*, *18*(2), 289–314. https://doi.org/10.1080/10705511.2011.557344

Word, E. R., Johnston, J., Bain, H. P., Fulton, B. D., Zaharias, J. B., Achilles, C. M., Lintz, M. N., Folger, J., & Breda, C. (1990). The State of Tennessee's Student/Teacher Achievement Ratio (STAR) Project: Technical Report (1985-1990). (tech. rep.) (ERIC Number: ED328356).

## Appendix I. Time coding transformations with latent interactions

### *Parameter estimate transformations*

Prior work (Biesanz et al., 2004) defined a transformation matrix to compute the results for an alternative coding scheme of time such that

$$\mathbf{T}^{-1} = \left(\mathbf{\Lambda}^{*'}\mathbf{\Lambda}^{*}\right)^{-1}\mathbf{\Lambda}^{*'}\mathbf{\Lambda} \tag{A1.1}$$

Taking advantage of the likelihood equivalence between different time coding solutions, Biesanz et al. (2004) further showed that because

$$\mathbf{\Lambda}^{*}\mathbf{\Psi}^{*}\mathbf{\Lambda}^{*} = \mathbf{\Lambda}\mathbf{\Psi}\mathbf{\Lambda} \quad \text{and} \quad \mathbf{\Lambda}^{*}\boldsymbol{\alpha}^{*} = \mathbf{\Lambda}\boldsymbol{\alpha} \tag{A1.2}$$

then

$$\mathbf{\Psi}^{*} = \mathbf{T}^{-1}\mathbf{\Psi}\mathbf{T}^{-1'} \quad \text{and} \quad \boldsymbol{\alpha}^{*} = \mathbf{T}^{-1}\boldsymbol{\alpha} \tag{A1.3}$$

We also outlined in McCormick et al. (2024) that a similar approach can be used to show that for the matrix $\mathbf{B}$ of distal outcome regressions

$$\mathbf{\Lambda}^{*}\mathbf{\Psi}^{*}\mathbf{B}^{*} = \mathbf{\Lambda}\mathbf{\Psi}\mathbf{B} \tag{A1.4}$$

such that

$$\mathbf{B}^{*} = \mathbf{T}'\mathbf{B} \tag{A1.5}$$

Because the repeated measures $y_{ti}$ are only connected to the distal outcome(s) $z_{pi}$ only through the latent factor structure, we derive the time coding-dependent parameter estimate changes straightforwardly. Consider the covariance between $y_{ti}$ and $z_{pi}$ in a model with latent endogenous interactions

$$\begin{aligned}\mathbf{\Sigma}_{yz} &= \mathbb{E}[yz] = \mathbb{E}\left[\left(\mathbf{\Lambda}\boldsymbol{\eta} + \boldsymbol{\varepsilon}_{y}\right)\left(\boldsymbol{\eta}'\mathbf{B} + \boldsymbol{\eta}'\mathbf{\Upsilon}\,\boldsymbol{\eta} + \boldsymbol{\varepsilon}_{z}\right)\right] \\ &= \mathbb{E}\left[\left(\mathbf{\Lambda}\boldsymbol{\eta} + \boldsymbol{\varepsilon}_{y}\right)\left(\boldsymbol{\eta}'\mathbf{B} + \boldsymbol{\eta}'\mathbf{\Upsilon}\left(\boldsymbol{\alpha} + \boldsymbol{\zeta}\right) + \boldsymbol{\varepsilon}_{z}\right)\right] \\ &= \left(\mathbf{\Lambda}\boldsymbol{\eta}\right)\left(\boldsymbol{\eta}'\mathbf{B} + \boldsymbol{\eta}'\mathbf{\Upsilon}\,\boldsymbol{\alpha}\right) = \mathbf{\Lambda}\mathbf{\Psi}\mathbf{B} + \mathbf{\Lambda}\mathbf{\Psi}\mathbf{\Upsilon}\,\boldsymbol{\alpha} \\ &= \mathbf{\Lambda}\mathbf{\Psi}\left(\mathbf{B} + \mathbf{\Upsilon}\,\boldsymbol{\alpha}\right)\end{aligned} \tag{A1.6}$$

So alternative time coding models must satisfy the equality

$$\mathbf{\Lambda}^{*}\mathbf{\Psi}^{*}\left(\mathbf{B}^{*} + \mathbf{\Upsilon}^{*}\boldsymbol{\alpha}^{*}\right) = \mathbf{\Lambda}\mathbf{\Psi}\left(\mathbf{B} + \mathbf{\Upsilon}\,\boldsymbol{\alpha}\right) \tag{A1.7}$$

allowing us to solve for $\mathbf{\Upsilon}^{*}$ using Equation A1.3 and A1.5, detailed below

$$\begin{aligned}&\left(\mathbf{\Lambda}\mathbf{T}\right)\left(\mathbf{T}^{-1}\mathbf{\Psi}\mathbf{T}^{-1'}\right)\left(\left[\mathbf{T}'\mathbf{B}\right] + \mathbf{\Upsilon}^{*}\left[\mathbf{T}^{-1}\boldsymbol{\alpha}\right]\right) = \mathbf{\Lambda}\mathbf{\Psi}\left(\mathbf{B} + \mathbf{\Upsilon}\,\boldsymbol{\alpha}\right) \\ &\mathbf{\Lambda}\mathbf{\Psi}\mathbf{B} + \mathbf{\Lambda}\mathbf{\Psi}\mathbf{T}^{-1'}\mathbf{\Upsilon}^{*}\mathbf{T}^{-1}\boldsymbol{\alpha} = \mathbf{\Lambda}\mathbf{\Psi}\mathbf{B} + \mathbf{\Lambda}\mathbf{\Psi}\mathbf{\Upsilon}\,\boldsymbol{\alpha} \\ &\mathbf{\Lambda}\mathbf{\Psi}\mathbf{T}^{-1'}\mathbf{\Upsilon}^{*}\mathbf{T}^{-1}\boldsymbol{\alpha} = \mathbf{\Lambda}\mathbf{\Psi}\mathbf{\Upsilon}\,\boldsymbol{\alpha} \\ &\mathbf{T}^{-1'}\mathbf{\Upsilon}^{*}\mathbf{T}^{-1} = \mathbf{\Upsilon}\end{aligned} \tag{A1.8}$$

which results in

$$\mathbf{\Upsilon}^{*} = \mathbf{T}'\mathbf{\Upsilon}\,\mathbf{T} \tag{A1.9}$$

Using this transformation also allows us to obtain the scalar equations for each individual parameter, recapitulating Equation 26

$$\begin{aligned}\mathbf{\Upsilon}^{*} = \mathbf{T}'\mathbf{\Upsilon}\,\mathbf{T} &= \begin{bmatrix}1 & 0 & 0\\ a & b & 0\\ 0 & 0 & 0\end{bmatrix}\begin{bmatrix}\upsilon_{11} & \upsilon_{12} & 0\\ 0 & \upsilon_{22} & 0\\ 0 & 0 & 0\end{bmatrix}\begin{bmatrix}1 & a & 0\\ 0 & b & 0\\ 0 & 0 & 0\end{bmatrix} \\ &= \begin{bmatrix}\upsilon_{11} & \upsilon_{11}a + \upsilon_{12}b & 0\\ \upsilon_{11}a & \upsilon_{11}a^{2} + \upsilon_{12}ab + \upsilon_{22}b^{2} & 0\\ 0 & 0 & 0\end{bmatrix}\end{aligned} \tag{A1.10}$$

which we can simplify in various ways (e.g., when $b = 1$ and/or $\upsilon_{11} = 0$).

### Standard error transformations

The standard errors of the transformed results can also be straightforwardly obtained. Prior work (Biesanz et al., 2004; Curran et al., 2004; McCormick et al., 2024) outlined how to obtain the Jacobian matrix of partial derivatives for the covariance matrix of the latent factors

$$\begin{aligned}\mathbf{J}_{vec(\boldsymbol{\Psi})\rightarrow vec(\boldsymbol{\Psi}^*)} &= \left[\frac{\delta vec(\boldsymbol{\Psi}^*)}{\delta vec(\boldsymbol{\Psi})}\right]' \\ &= \left[\frac{\delta(\mathbf{T}^{-1}\otimes\mathbf{T}^{-1})vec(\boldsymbol{\Psi})}{\delta vec(\boldsymbol{\Psi})}\right]' \\ &= (\mathbf{T}^{-1}\otimes\mathbf{T}^{-1})'\end{aligned} \tag{A1.11}$$

and the matrix of distal outcome regressions

$$\begin{aligned}\mathbf{J}_{vec(\mathbf{B})\rightarrow vec(\mathbf{B}^*)} &= \left[\frac{\delta vec(\mathbf{B}^*)}{\delta vec(\mathbf{B})}\right]' \\ &= \left[\frac{\delta vec(\mathbf{T}'\mathbf{B})}{\delta vec(\mathbf{B})}\right]' \\ &= [\mathbf{T}']' \\ &= \mathbf{T}\end{aligned} \tag{A1.12}$$

such that

$$\text{ACOV}(\boldsymbol{\Psi}^*) = \mathbf{J}'_{vec(\boldsymbol{\Psi})\rightarrow vec(\boldsymbol{\Psi}^*)}\text{ACOV}(\boldsymbol{\Psi})\mathbf{J}_{vec(\boldsymbol{\Psi})\rightarrow vec(\boldsymbol{\Psi}^*)} \tag{A1.13}$$

and

$$\begin{aligned}\text{ACOV}(\mathbf{B}^*) &= \mathbf{J}'_{vec(\mathbf{B})\rightarrow vec(\mathbf{B}^*)}\text{ACOV}(\mathbf{B})\mathbf{J}_{vec(\mathbf{B})\rightarrow vec(\mathbf{B}^*)} \\ &= \mathbf{T}'\text{ACOV}(\mathbf{B})\mathbf{T}\end{aligned} \tag{A1.14}$$

Applying the same procedure to the matrix of interaction effects $\boldsymbol{\Upsilon}$, we can see that

$$\begin{aligned}\mathbf{J}_{vec(\boldsymbol{\Upsilon})\rightarrow vec(\boldsymbol{\Upsilon}^*)} &= \left[\frac{\delta vec(\boldsymbol{\Upsilon}^*)}{\delta vec(\boldsymbol{\Upsilon})}\right]' \\ &= \left[\frac{\delta(\mathbf{T}\otimes\mathbf{T})vec(\boldsymbol{\Upsilon})}{\delta vec(\boldsymbol{\Upsilon})}\right]' \\ &= (\mathbf{T}\otimes\mathbf{T})'\end{aligned} \tag{A1.15}$$

such that

$$\text{ACOV}(\boldsymbol{\Upsilon}^*) = \mathbf{J}'_{vec(\boldsymbol{\Upsilon})\rightarrow vec(\boldsymbol{\Upsilon}^*)}\text{ACOV}(\boldsymbol{\Upsilon})\mathbf{J}_{vec(\boldsymbol{\Upsilon})\rightarrow vec(\boldsymbol{\Upsilon}^*)} \tag{A1.16}$$

With standard errors being obtained by taking the square root of the diagonal of the resulting matrix $\text{ACOV}(\boldsymbol{\Upsilon}^*)$.

## Appendix II. Expanded transformations in nonlinear models and models with multiple distal outcomes

For simplicity, the main results—as in McCormick et al. (2024)—consider the case of the linear growth model with a single distal outcome. However, the **matrix** expressions derived in this treatment generalize readily to contexts of nonlinear polynomial growth models, and to models with more than a single distal outcome. Below, I outline how these transformations follow the same expressions as before.

### Time coding derivations in the quadratic growth model

In the quadratic model, the factor loading matrix $\boldsymbol{\Lambda}$ is expanded to contain squared factor loadings. For instance, the quadratic version of Equation 3 would be

$$\boldsymbol{\Lambda}_{\text{quad}} = \begin{bmatrix} 1 & 0 & 0 & 0 \\ 1 & 1 & 1 & 0 \\ 1 & 2 & 4 & 0 \\ 1 & 3 & 9 & 0 \\ 1 & 4 & 16 & 0 \\ 0 & 0 & 0 & 1 \end{bmatrix} \tag{A2.1}$$

with a matrix of distal outcome regressions $\mathbf{B}$ from Equation 4 as

$$\mathbf{B}_{\text{quad}} = \begin{bmatrix} 0 & 0 & 0 & 0 \\ 0 & 0 & 0 & 0 \\ \beta_{z_1,\eta_1} & \beta_{z_1,\eta_2} & \beta_{z_1,\eta_3} & 0 \end{bmatrix} \tag{A2.2}$$

To accomplish time coding transformations in expanded polynomial models, we can also expand the transformation matrix $\mathbf{T}$ to include an additional column. This would have the form

$$\mathbf{T}_{\text{quad}} = \begin{bmatrix} 1 & a & a^2 & 0 \\ 0 & b & 2ab & 0 \\ 0 & 0 & b^2 & 0 \\ 0 & 0 & 0 & 1 \end{bmatrix} \tag{A2.3}$$

with a quadratic expression of the $a$ and $b$ shift and scaling parameters in the quadratic column. However, deriving these elements individually is not necessary, as they can be computed directly from the expression in Equation A1.1, which only requires that we know the factor loading matrix of the original ($\boldsymbol{\Lambda}$) and target ($\boldsymbol{\Lambda}^*$) model. Once we have this transformation matrix $\mathbf{T}$, all of the same transformation expressions from Appendix I hold. Indeed this is the true advantage of adopting matrix, rather than scalar, expressions for these transformations. A demonstration of these expressions can be seen in the Supplemental Material.

### Time coding derivations with multiple distal outcomes

Expanding the model to include multiple distal outcomes into the model involves similarly straightforward expansions of the $\boldsymbol{\Psi}$ and $\mathbf{B}$ matrices. The resulting equations expand on Equations 3 and 4, with additional rows and columns for a second distal outcome, including in the measurement

$$\begin{bmatrix} y_{1i} \\ y_{2i} \\ y_{3i} \\ y_{4i} \\ y_{5i} \\ z_{1i} \\ z_{2i} \end{bmatrix} = \begin{bmatrix} 1 & 0 & 0 & 0 \\ 1 & 1 & 0 & 0 \\ 1 & 2 & 0 & 0 \\ 1 & 3 & 0 & 0 \\ 1 & 4 & 0 & 0 \\ 0 & 0 & 1 & 0 \\ 0 & 0 & 0 & 1 \end{bmatrix} \begin{bmatrix} \eta_{1i} \\ \eta_{2i} \\ \eta_{z_1 i} \\ \eta_{z_2 i} \end{bmatrix} + \begin{bmatrix} \varepsilon_{1i} \\ \varepsilon_{2i} \\ \varepsilon_{3i} \\ \varepsilon_{4i} \\ \varepsilon_{5i} \\ \varepsilon_{z_1 i} \\ \varepsilon_{z_2 i} \end{bmatrix} \tag{A2.4}$$

and structural

$$\begin{bmatrix} \eta_{1i} \\ \eta_{2i} \\ \eta_{z_1 i} \\ \eta_{z_2 i} \end{bmatrix} = \begin{bmatrix} \alpha_1 \\ \alpha_2 \\ \alpha_{z_1} \\ \alpha_{z_2} \end{bmatrix} + \begin{bmatrix} 0 & 0 & 0 & 0 \\ 0 & 0 & 0 & 0 \\ \beta_{z_1,\eta_1} & \beta_{z_1,\eta_2} & 0 & 0 \\ \beta_{z_2,\eta_1} & \beta_{z_2,\eta_2} & 0 & 0 \end{bmatrix} \begin{bmatrix} \eta_{1i} \\ \eta_{2i} \\ \eta_{z_1 i} \\ \eta_{z_2 i} \end{bmatrix} + \begin{bmatrix} \zeta_{1i} \\ \zeta_{2i} \\ \zeta_{z_1 i} \\ \zeta_{z_2 i} \end{bmatrix} \tag{A2.5}$$

model. The covariance matrix $\boldsymbol{\Psi}$ also expands, maintaining the block structure of covariances for the latent growth factors and distal outcome single-indicator factors (these cross-block covariance relationships are structured as regressions in $\mathbf{B}$).

$$\boldsymbol{\Psi} = \begin{bmatrix} \psi_{11} & \psi_{12} & 0 & 0 \\ \psi_{21} & \psi_{22} & 0 & 0 \\ 0 & 0 & \psi_{z_1} & \psi_{34} \\ 0 & 0 & \psi_{43} & \psi_{z_2} \end{bmatrix} \tag{A2.6}$$

The time coding transformation matrix $\mathbf{T}$ expands as well but changes little in terms of substantive structure

$$\mathbf{T} = \begin{bmatrix} 1 & a & 0 & 0 \\ 0 & b = 1 & 0 & 0 \\ 0 & 0 & 1 & 0 \\ 0 & 0 & 0 & 1 \end{bmatrix} \tag{A2.7}$$

Once we have these expanded matrices, all the same matrix expressions as before yield the correct time coding transformations across alternative placements of the intercept.